J. Fluid Mech. (2011), *vol.* 679, *pp.* 505–543.
doi:10.1017/jfm.2011.143

Energy transfer mechanism of the instability of an axisymmetric swirling flow in a finite-length pipe

S. WANG[1]† AND Z. RUSAK[2]

[1]Department of Mathematics, University of Auckland, 38 Princes Street, Auckland 1142, New Zealand

[2]Department of Mechanical, Aerospace, and Nuclear Engineering, Rensselaer Polytechnic Institute, Troy, NY 12180-3590, USA

(Received 27 March 2009; revised 14 December 2010; accepted 20 March 2011; first published online 25 May 2011)

The rate of change of the perturbation's kinetic energy E of a perturbed inviscid, incompressible, axisymmetric, columnar and near-critical swirling flow in a finite-length, straight, circular pipe with periodic and non-periodic inlet–outlet conditions is studied using the Reynolds–Orr equation. The perturbation's mode shape and growth rate are computed from the linear-stability eigenvalue problem using a novel asymptotic solution in the case of a flow in a long pipe. This solution technique is general and can be applied to any vortex flow profile, in a range of swirl levels around the critical level, and for various boundary conditions. The solutions are used to analytically estimate the production (or loss) of E at the pipe boundaries and inside the domain and to shed new light on the Wang–Rusak mechanism of exchange of global stability around the critical swirl, that is leading to the vortex breakdown process. It is shown that the production of E inside the domain is modulated by the base flow strain-rate tensor. For the special case of a solid-body rotating flow, this term vanishes and the stability is determined only by the asymmetric transfer of E at the boundaries. For a general base flow, the dominant perturbation's mode shape develops deviations in response to the non-periodic inlet–outlet conditions. These deviations couple with the base flow strain-rate tensor to generate production or loss of E in the bulk. Together with the asymmetric transfer of E at the boundaries, they form a critical balance of production of E and determine the flow stability around the critical state. This behaviour is demonstrated for the Lamb–Oseen and Q vortex models. This analysis reveals a more complicated, as well more realistic, interaction between the perturbed flow in the domain and at the boundaries that dominates vortex flow dynamics.

Key words: vortex breakdown, vortex instability

1. Introduction

The study of the stability of axisymmetric swirling flows in a pipe is a classical topic in fluid mechanics; see the excellent review papers on this topic by Leibovich (1984) and Ash & Khorrami (1995). Rayleigh (1916) and Synge (1933) established that an incompressible and inviscid, columnar, swirling flow in an infinitely long, straight, circular pipe, or equivalently in a finite-length pipe with periodic inlet–outlet

† Email address for correspondence: wang@math.auckland.ac.nz

conditions, is linearly neutrally stable with respect to axisymmetric perturbations if and only if the absolute value of the base flow circulation function $K(r)$ increases monotonically with the radius r from the centre, i.e. $\Phi = (1/r^3)\,\mathrm{d}(K^2)/\mathrm{d}r > 0$. Specifically, the solid-body rotating flow where $K = \omega r^2$ is always neutrally stable under the periodic conditions. Howard & Gupta (1962) extended this criterion to a vortex flow with an axial velocity profile $W(r)$. The flow is linearly neutrally stable with respect to axisymmetric perturbations if $\Phi > (\mathrm{d}W/\mathrm{d}r)^2/4$, reflecting the complex interaction and exchange of kinetic energy of perturbations with the base flow radial gradients. Leibovich & Stewartson (1983) used an asymptotic theory to derive a sufficient condition for vortex flow instability with respect to helical perturbations with high circumferential wavenumbers. This condition relates between the base flow strain rates. The numerical growth rate calculations of Lessen, Singh & Paillet (1974) and Mayer & Powell (1992) agree with this theory. When the vortex flow is stable according to the above criteria, classical vortex stability theory considers the vortex core as a neutral waveguide; see for example Gallaire & Chomaz (2004) and Fabre, Sipp & Jacquin (2006) for insightful discussions of the neutral or near-neutral Kelvin waves in the Lamb–Oseen vortex. However, the classical theory is limited to the evolution of axially periodic perturbations and may not describe the actual flow physics in vortex tubes of a finite length where the effect of non-periodic inlet–outlet conditions can generate perturbation modes that are different from the axially periodic waves.

Motivated by the vortex breakdown phenomenon, Squire (1960) and Benjamin (1962) studied the nature of the family of columnar, axisymmetric swirling flows in an infinitely long pipe with zero radial velocity and circumferential and axial velocities, $V = \omega v_0(r)$ and $W = w_0(r)$ respectively, that depend only on the radial distance r. Here ω is the flow swirl ratio and v_0 and w_0 are the base flow profiles. These states constitute a branch of base solutions of the steady, incompressible, inviscid and axisymmetric flow equations. Along this branch of states they identified a certain critical level of swirl, denoted as ω_B, where an infinitely long infinitesimal axisymmetric standing wave may first appear as the swirl ratio ω is increased. The critical-state theory of Benjamin (1962) relates the dynamical characteristics of a swirling columnar flow to its ability to sustain standing axisymmetric small-disturbance waves. Supercritical vortex flows have swirl ratios below ω_B and allow only downstream propagating waves while subcritical flows have swirl ratios above ω_B and allow the upstream and downstream propagation of waves. Benjamin (1962) also used a variational principle for the flow equations and described the axisymmetric breakdown as a transition from an upstream supercritical columnar vortex flow to a downstream subcritical columnar flow. It should be noted that Benjamin (1962) did not establish any relationship between criticality and stability of vortex flows.

In a recent study, Wang (2009) has proved the nonlinear stability to finite-amplitude, axisymmetric perturbations for any columnar vortex flow in an infinitely long pipe that satisfies Rayleigh's criterion. Moreover, an upper bound of the disturbance's kinetic energy E has been obtained in terms of the base flow properties and the initial kinetic energy of the disturbance. This upper bound is valid for any initial disturbance with a finite amplitude, and thus characterizes the maximum potential for disturbance growth. It should also be noted that this upper bound does not depend on the vortex swirl level at all. The nonlinear stability analysis of Wang (2009) shows that flow criticality is not related at all to the flow stability characteristics in an infinitely long pipe setting, i.e. disturbances can propagate either upstream or downstream but are subject to the same upper bound of disturbance amplitude growth. This is in agreement with the translation-invariant nature of the problem.

Recent studies have revealed that vortices can also support the transient growth of waves to significant amplitudes (see Schmid & Henningson 2001 for transient growth phenomena and Antkowiak & Brancher 2004, Pradeep & Hussain 2006 and Heaton & Peake 2007 for transient growth in vortices). This behaviour stems from the non-orthogonal nature of the eigenmodes, which induces a strong coupling among the eigenmodes. For axisymmetric disturbances, the transient growth, or any type of growth of whatever physical nature, must obey the upper bound obtained from the nonlinear stability analysis of Wang (2009). It can be shown that for the Lamb–Oseen vortex with a moderate size of vortex core, the disturbance's growth is limited to relatively small values. Thus, small disturbances in such flows would never develop into a vortex breakdown state. This is in contrast to results from direct numerical simulations that show the breakdown of such flows above a certain level of swirl (see, for example, Rusak, Wang & Whiting 1998). Thus, there is a definite need to choose an adequate physical model, different from the setting of a flow in an infinitely long pipe, in the study of the vortex breakdown phenomenon.

Wang & Rusak (1996, hereinafter referred to as WR, to avoid the ambiguity with the classical Rayleigh instability) studied the stability of an inviscid and incompressible, columnar, axisymmetric swirling flow in a finite-length pipe with certain non-periodic boundary conditions imposed at the pipe inlet and outlet. These conditions model the physical situation of a flow in a long pipe that is generated by a vortex generator ahead of the pipe inlet at continuous and smooth operation. They found that these boundary conditions impose a dramatic change on the stability characteristics of a swirling flow and related for the first time the stability and criticality of a vortex flow. Using a novel analytical solution of the perturbation's non-axially periodic mode shape and its growth rate, both are functions of the swirl ratio, they proved for the first time that the solid-body rotating flow is unstable at swirl ratios ω above a critical level ω_1. Here ω_1 is the corrected critical swirl of Benjamin (1962) for a finite-length pipe. Note that ω_1 approaches ω_B as pipe length increases. Moreover, they showed that general vortex flows, including flows that are stable according to the criterion of Rayleigh (1916) and Synge (1933) as well as according to all previously known criteria, develop an instability at swirl ratios ω above their respective critical swirl ω_1. The instability discovered in WR (hereinafter referred to as the WR instability) is a result of the interaction between swirl-driven azimuthal vorticity waves propagating upstream, the base flow axial speed convecting disturbances downstream, and the relatively fixed pipe inlet conditions. These interactions create a critical balance at ω_1. Therefore, the dynamical meaning of the critical swirl ω_1 is the same as that of ω_B. When $\omega < \omega_1$ (the supercritical swirl region) small-disturbance waves are convected out of the finite domain, leading to the asymptotic decay of the perturbation in time. At the critical state $\omega = \omega_1$, a neutral standing wave appears. However, when $\omega > \omega_1$ (the subcritical swirl region) the waves propagate upstream towards the inlet, are trapped near the inlet, accumulate, and therefore grow exponentially in time (this is very much like the initiation of buckling of a beam in structures mechanics). This stability analysis has also shown for the first time that boundary conditions (the non-symmetric inlet–outlet conditions) have an important role in the stability of swirling flows. This type of stability is referred to as *global stability* to emphasize the influence of the boundary conditions at the pipe inlet and outlet on the base flow stability.

It is therefore clear that the classical Rayleigh's stability criterion is closely tied to the periodic inlet–outlet conditions. From a physical point of view, in the case of an axisymmetric swirling flow in an infinitely long, straight, circular pipe, or in a finite-length pipe with periodic inlet–outlet conditions, the disturbance is free to propagate

upstream and downstream along the vortex core, making the core a waveguide. However, when non-periodic boundary conditions are imposed in a finite-length pipe, the propagation of the disturbance is not as free as it is in an infinitely long pipe. In this case the translation-invariant nature of the flow does not exist any more. As a consequence, flow criticality has a dominant influence over the flow stability characteristics. As shown in the present paper, the kinetic energy transfer mechanism between the dominant disturbance and the base flow at swirl levels around the critical swirl ω_1 is strongly affected by the non-periodic boundary conditions.

Wang & Rusak (1997*a*) also conducted a global analysis of the dynamics of swirling flow in a pipe and showed the relationship between the instability mechanism (WR) and the initiation of the axisymmetric vortex breakdown process, leading to the development of axisymmetric vortex breakdown states. This mechanism was also demonstrated by Rusak *et al.* (1998) using direct numerical simulations of the complex evolution of vortex states in a pipe with inlet flows described by the Lamb–Oseen (Burgers) vortex. The effect of real flow parameters such as slight viscosity in high-Reynolds-number flows (Wang & Rusak 1997*b*), small pipe divergence (Rusak & Judd 2001), inlet azimuthal vorticity (Rusak 1998) and weak chemical reaction (Rusak, Kapila & Choi 2002) on the dynamics of general vortex flows was also studied. All these effects act as physical perturbations and can exist in experimental flow apparatuses. They modify the transcritical bifurcation of solutions of an inviscid, incompressible, non-reacting, swirling flow in a straight circular pipe into branches of non-columnar states with folds at modified critical (limit) swirl levels. These fold points inherit the properties of the critical swirl ω_1 and were shown to be points of exchange of stability along the modified branches of vortex states with a modified mode of perturbation of the mode found in WR (see, for example, the stability analysis of Rusak & Judd 2001 of vortex states in a slightly diverging pipe). In addition, the linear and global bifurcation and stability analysis of compressible vortex flows in a pipe also show (Rusak & Lee 2002, 2004; Rusak, Choi & Lee 2007) the further complex interaction of the azimuthal vorticity waves with acoustic and entropy waves resulting from the coupling between swirl and temperature gradients (baroclinic effects) and with the fixed inlet conditions. It leads to a modified dynamic behaviour of vortex flows at subsonic speeds, which is inherited from the incompressible flow behaviour. The critical swirl ω_1 increases with the increase of the flow subsonic Mach number, yet the exchange of stability at ω_1 is similar to that found by WR. It should be noted that all of these studies also show that the incompressible, solid-body rotation is a special flow with a jump bifurcation at the critical swirl to breakdown states. This jump behaviour is sensitive to perturbations including real flow effects and is modified by these effects to that of a general swirling flow behaviour.

The WR instability is fundamentally different from all the classical vortex stability mechanisms. In this paper, we look to shed more light on the underlying physical mechanism behind this instability. Specifically, we focus on identifying the kinetic energy balance between the base flow and the perturbation and from where the disturbance gains the energy to sustain the exponential growth at swirl ratios above the critical level (in the subcritical region of swirl). For incompressible flows, the kinetic energy of perturbations, E, provides a non-negative quantitative measure of the perturbation's size. The rate of change of E in time is described according to the classical Reynolds–Orr equation (see the review by Wu, Ma & Zhou 2006), modified to include the boundaries effect. Note that this fundamental equation shows that $\mathrm{d}E/\mathrm{d}t$ is determined by production terms of E inside the flow domain and at the pipe boundaries. The production of E inside the domain is modulated by the base flow

strain-rate tensor. We compute the various production terms and then highlight the exchange of kinetic energy between the perturbations and the base flow in the various parts of the pipe as swirl ratio is increased. This approach provides an energy-based mechanism for the formation of the WR instability as swirl ratio increases around the critical level from the supercritical region to the subcritical region.

We comment here that the strain-free nature of the solid-body rotation results in no production of E inside the domain, and thereby creates a decoupling of the kinetic energy of the perturbation from the base flow properties. This is a well-known fact and was used by Drazin (2002) to show the stability of the solid-body rotation in a straight pipe with periodic inlet–outlet conditions with respect to finite-amplitude perturbations. When non-periodic conditions are imposed in a finite-length pipe and the WR instability arises for swirl ratios above the critical level, the necessary energy to sustain the perturbation's exponential growth must therefore be gained by the energy production at the inlet and outlet. Recently, Gallaire & Chomaz (2004) considered this problem by studying the solid-body rotation in a finite-length, straight, circular pipe. They described the perturbation's mode shape and, through integration by parts of E, found that the disturbance gains or loses its kinetic energy only at the boundaries of the pipe as swirl is increased around the critical level ω_1. In this special case, the vortex core serves again as a neutral waveguide, convecting the perturbations from the inlet to the outlet without affecting their size. Here the difference between the inlet and outlet production terms determines the WR instability. Gallaire, Chomaz & Huerre (2004) developed an optimal linear control approach to delay the onset of instability of the solid-body rotation at ω_1 to higher values.

In this paper, we study the rate of change of the perturbation's kinetic energy E of a perturbed inviscid, axisymmetric, and near-critical swirling flow in a finite-length, straight, circular pipe with periodic and non-periodic inlet–outlet conditions. The mathematical model and the linear stability problem are described in § 2. The perturbation's mode shape and growth rate as a function of swirl ratio are computed in § 3 using a new asymptotic solution of the linear stability problem in the case of a long pipe where the eigenvalue problem is simplified. Results for the representative and physically relevant Lamb–Oseen and Q vortices are presented in a range of swirl levels around their respective critical levels and for various boundary conditions. The Reynolds–Orr equation for E is presented in § 4, including the production terms of E inside the domain and at the pipe inlet and outlet. The solutions of the perturbation's mode shape are used in § 5 to derive an asymptotic form of the Rayleigh–Orr equation. This form is further explored in § 6 to provide an asymptotic estimate of the production (or loss) of E at the pipe boundaries and inside the domain and to shed a new light on the WR mechanism of exchange of global stability around the critical swirl. In § 7, the physical interpretation of the results is discussed. The focus is on the basic mechanism of the global stability and its difference from the classical Rayleigh stability mechanism.

The present analysis shows that the production of E inside the domain is an important part of the WR instability mechanism. It is modulated by the base flow strain-rate tensor. For a relatively general base flow such as the Lamb–Oseen and Q vortices, the perturbation's mode shape develops a natural deviation with respect to the critical mode in response to the non-periodic inlet and outlet conditions at $x = 0$ and $x = L$, respectively (here x is the axial position along the pipe). This deviation couples with the base flow strain-rate tensor to generate production or loss of E inside the domain. The mode shape deviation also results in asymmetric production of E at the boundaries. These effects together form a critical balance of production of E from

the base flow and determine the flow stability around the critical state. This analysis reveals a more complicated and more realistic interaction between the perturbed flow inside the domain and at the boundaries that dominates vortex flow dynamics. The flow in the domain is active in not only convecting the perturbations as a waveguide from the inlet to the outlet but also affecting their size and growth rate by engaging with the base flow strain rates to produce (or lose) their kinetic energy. With this mechanism in mind, it is clear that real physical effects such as pipe divergence, slight viscosity, inlet vorticity disturbances and weak reaction also naturally add to the mode shape deviation and enhance the production of the perturbation's kinetic energy inside the domain. They alter the production of energy inside the domain and promote the onset of instability at swirl ratios below critical. On the other hand, real flow effects such as pipe contraction and compressibility increase the loss of energy in the bulk to delay the onset of the instability to swirl ratios above critical. These effects can be proved by similar analysis techniques.

2. Mathematical model and linear stability problem

We consider an axisymmetric, incompressible and inviscid flow in a straight, finite-length circular pipe. We use cylindrical coordinates (r, θ, x) where (u, v, w) are the radial, azimuthal and axial velocity components, respectively. In a dimensionless form, axial and radial distances are scaled with the pipe radius (that is set as unit) and pipe non-dimensional length is L. Velocity components are scaled with the characteristic axial speed entering the pipe. Time t is scaled with the ratio of pipe radius to inlet characteristic speed. Let $y = r^2/2$. By virtue of the axisymmetry, a streamfunction $\psi(x, y, t)$ can be defined such that $u = -\psi_x/\sqrt{2y}$ and $w = \psi_y$. The reduced form of azimuthal vorticity is $\chi = -(\psi_{yy} + \psi_{xx}/2y)$ (where the azimuthal vorticity is $\eta = \sqrt{2y}\chi$). The circulation function $K(x, y, t)$ is defined as $K = rv = \sqrt{2y}v$.

The equations which relate the evolution of $\psi(x, y, t)$, $\chi(x, y, t)$ and $K(x, y, t)$ can be written in a compact form (see for example Szeri & Holmes 1988) as

$$\left.\begin{aligned} K_t + \{\psi, K\} &= 0, \\ \chi_t + \{\psi, \chi\} &= \frac{1}{4y^2}(K^2)_x, \end{aligned}\right\} \tag{2.1}$$

where the bracket $\{f, g\}$ is the canonical Poisson bracket or Jacobian defined as

$$\{f, g\} = f_y g_x - f_x g_y. \tag{2.2}$$

The first equation in (2.1) describes the transport of circulation along a flow pathline. The second equation describes the interaction between the convection of the reduced azimuthal vorticity χ along a pathline and vorticity stretching by the axial gradient of the circulation. The latter effect is swirl dependent and generates swirl-driven waves that can move either downstream or upstream towards the inlet.

We study the dynamics of the vortex flow in the pipe under the certain conditions imposed on the boundaries to reflect a physical setting of a flow in a pipe generated by a vortex generator ahead of the pipe that is at a steady and continuous operation. In this setting, the profiles of the axial and circumferential velocity components as well as the azimuthal vorticity at the exit of the vortex generator and that enter the pipe at $x = 0$ are assumed to be fixed for all time t and smooth in y, i.e. we assume that for all time $t \geqslant 0$ and for $0 \leqslant y \leqslant 1/2$, $\psi(0, y, t) = \psi_0(y)$ and $K(0, y, t) = \omega K_0(y)$ are given at the pipe inlet. Here $\omega \geqslant 0$ is the base flow swirl ratio, $\psi_0(y)$ is the inlet volumetric flux profile and $K_0(y)$ is the inlet circulation profile, rescaled with ω. These

functions must satisfy the symmetry conditions at $y=0$, $\psi_0(0)=0$ and $K_0(0)=0$. We also set $\psi_{xx}(0, y, t)=0$ to fix the reduced azimuthal vorticity to be $\chi(0, y, t)=-\psi_{0yy}$ along the inlet for all time t and $0\leqslant y\leqslant 1/2$. For the steady-state case, this set of pipe inlet conditions describes for all ω a total head conserving apparatus which can be physically realized (see the discussion in Appendix A).

At the pipe outlet $x=L$, two types of conditions may be considered. The first possible outlet condition refers to a sufficiently long pipe (where $L\gg 1$) and describes an expected fully developed columnar state with zero radial velocity, i.e. for all time t, $\psi_x(L, y, t)=0$ for $0\leqslant y\leqslant 1/2$. This outlet condition was used in the stability analysis of WR. The second possible outlet condition refers to pipes with a discharge device. Then, a more relevant boundary condition at the pipe outlet may fix the flow flux profile, i.e. for all time t, $\psi(L, y, t)=\psi_0(y)$ for $0\leqslant y\leqslant 1/2$. In this paper, we study the flow stability under either one of these two possible outlet conditions. In addition, along the pipe centreline at $y=0$ the symmetry condition is imposed, i.e. $\psi(x, 0, t)=0$ for $0\leqslant x\leqslant L$ and for all time $t\geqslant 0$. Along the pipe wall at $y=1/2$ the streamfunction is fixed $\psi(x, 1/2, t)=\psi_0(1/2)$ for $0\leqslant x\leqslant L$ and for all time $t\geqslant 0$ to describe the total volumetric flux $\psi_0(1/2)$ across the pipe and the flow tangency along the pipe wall.

We consider a steady, columnar (x independent) base flow solution of (2.1) where, for all incoming swirl levels ω, the velocity components are functions of y only, i.e.

$$u=U(y)=0,\quad v=V(y)=\omega v_0(y),\quad w=W(y)=w_0(y). \tag{2.3}$$

From (2.3) we find that the base flow is characterized by $\psi=\psi_0(y)=\int_0^y w_0(y')\,\mathrm{d}y'$, $\chi=\chi_0(y)=-w_{0y}=-\psi_{0yy}$ and $K=\omega K_0(y)=\omega\sqrt{2y}v_0(y)$.

To study the linear stability of this flow, an infinitesimal unsteady streamfunction disturbance $\psi_1(x, y, t)$ and a circulation disturbance $K_1(x, y, t)$ are superimposed on the base flow functions:

$$\left.\begin{aligned}\psi(x, y, t)&=\psi_0(y)+\epsilon_1\psi_1(x, y, t)+\cdots,\\ K(x, y, t)&=\omega K_0(y)+\epsilon_1 K_1(x, y, t)+\cdots,\end{aligned}\right\} \tag{2.4}$$

with $0\leqslant\epsilon_1\ll 1$. Then, $\chi(x, y, t)=-\psi_{0yy}+\epsilon\chi_1(x, y, t)+\cdots$ and $\chi_1=-(\psi_{1yy}+\psi_{1xx}/2y)$ is the disturbance of the reduced azimuthal vorticity. On substituting these expressions into (2.1) and neglecting the second-order perturbation terms, one obtains at order $O(\epsilon_1)$ the linearized equations of motion relating ψ_1, χ_1 and K_1:

$$\left.\begin{aligned}K_{1t}+\psi_{0y}K_{1x}-\omega K_{0y}\psi_{1x}&=0,\\ \chi_{1t}+\psi_{0y}\chi_{1x}+\psi_{0yyy}\psi_{1x}&=\frac{\omega K_0}{2y^2}K_{1x}.\end{aligned}\right\} \tag{2.5}$$

From the boundary conditions set above, we have for all $t\geqslant 0$ at order $O(\epsilon_1)$ the linearized boundary conditions for ψ_1 and K_1:

$$\left.\begin{aligned}&\psi_1(x, 0, t)=0, \quad \psi_1(x, 1/2, t)=0 \quad \text{for } 0\leqslant x\leqslant L,\\ &\psi_1(0, y, t)=0, \quad \phi_{1xx}(0, y, t)=0, \quad K_1(0, y, t)=0 \quad \text{for } 0\leqslant y\leqslant 1/2,\\ &\psi_{1x}(L, y, t)=0 \quad \text{or } \psi_1(L, y, t)=0 \quad \text{for } 0\leqslant y\leqslant 1/2.\end{aligned}\right\} \tag{2.6}$$

We introduce mode analysis of (2.5) and (2.6) of the form

$$\left.\begin{aligned}\psi_1(x, y, t)&=\phi(x, y;\sigma)\,\mathrm{e}^{\sigma t},\\ K_1(x, y, t)&=k(x, y;\sigma)\,\mathrm{e}^{\sigma t}.\end{aligned}\right\} \tag{2.7}$$

Here σ is the non-dimensional growth rate. From (2.5) and (2.7), we obtain the linear stability equation for the solution of σ and $\phi(x, y; \sigma)$:

$$\left(\phi_{yy} + \frac{\phi_{xx}}{2y} + \left(\Omega \frac{K_0 K_{0y}}{2y^2 \psi_{0y}^2} - \frac{\psi_{0yyy}}{\psi_{0y}}\right)\phi\right)_{xx} - \frac{\sigma \psi_{0yyy}}{\psi_{0y}^2}\phi_x + \frac{2\sigma}{\psi_{0y}}\left(\phi_{yy} + \frac{\phi_{xx}}{2y}\right)_x + \frac{\sigma^2}{\psi_{0y}^2}\left(\phi_{yy} + \frac{\phi_{xx}}{2y}\right) = 0. \quad (2.8)$$

Here $\Omega = \omega^2$ is a modified swirl parameter. For the detailed derivation of (2.8), see WR.

From the conditions (2.6), the corresponding boundary conditions for ϕ and k are

$$\left.\begin{array}{lll} \phi(x, 0; \sigma) = 0, & \phi(x, 1/2; \sigma) = 0 & \text{for } 0 \leqslant x \leqslant L, \\ \phi(0, y; \sigma) = 0, & \phi_{xx}(0, y; \sigma) = 0, & k(0, y; \sigma) = 0 \quad \text{for } 0 \leqslant y \leqslant 1/2, \\ \phi_x(L, y; \sigma) = 0 & \text{or } \phi(L, y; \sigma) = 0 & \text{for } 0 \leqslant y \leqslant 1/2. \end{array}\right\} \quad (2.9)$$

The inlet condition $k(0, y; \sigma) = 0$ can be replaced by (see details in WR)

$$\phi_{yyx}(0, y; \sigma) + \frac{\phi_{xxx}(0, y; \sigma)}{2y} + \left(\Omega \frac{K_0 K_{0y}}{2y^2 \psi_{0y}^2} - \frac{\psi_{0yyy}}{\psi_{0y}}\right)\phi_x(0, y; \sigma) = 0. \quad (2.10)$$

3. Novel asymptotic solution of vortex linear stability problem for a long pipe

3.1. *Model linear stability problem for a swirling flow in a long pipe*

Let $\epsilon = 1/L^2$. In the case of a long pipe where $L \gg 1$, $0 < \epsilon \ll 1$. The stability problem (2.8), (2.9) and (2.10) may have the following asymptotic solution:

$$\phi(x, y; \sigma) = \phi_B(y) A(X; \sigma^*) + \epsilon \bar{\phi}(X, y; \sigma^*) + O(\epsilon^2). \quad (3.1)$$

Here $X = \sqrt{\epsilon} x$ and then the rescaled pipe length is $X_0 = \sqrt{\epsilon} L = 1$. Also, $\sigma^* = \sigma/\epsilon^{3/2}$, $\Omega = \Omega_B + \Delta\Omega$, $\Delta\Omega = \kappa_\omega \epsilon$, and $\Omega_B = \omega_B^2$ and $\phi_B(y)$ are the square of Benjamin's critical swirl and related eigenmode, respectively, and both result from the solution of the first eigenvalue of the problem:

$$\left.\begin{array}{r} \phi_{Byy} + \left(\Omega_B \dfrac{K_0 K_{0y}}{2y^2 \psi_{0y}^2} - \dfrac{\psi_{0yyy}}{\psi_{0y}}\right)\phi_B = 0, \\ \phi_B(0) = \phi_B(1/2) = 0. \end{array}\right\} \quad (3.2)$$

We first analyse the boundary conditions (2.9) and (2.10) of the problem. From (2.9) and asymptotic solution (3.1), the function $A(X; \sigma^*)$ must satisfy the inlet conditions $A(0; \sigma^*) = 0$, $A_{XX}(0; \sigma^*) = 0$ and either $A_X(1; \sigma^*) = 0$ or $A(1; \sigma^*) = 0$ outlet condition. Also, the function $\bar{\phi}(X, y; \sigma^*)$ must satisfy

$$\left.\begin{array}{lll} \bar{\phi}(0, y; \sigma^*) = 0, & \bar{\phi}_{XX}(0, y; \sigma^*) = 0 & \text{for } 0 \leqslant y \leqslant 1/2, \\ \bar{\phi}_X(1, y; \sigma^*) = 0 & \text{or } \bar{\phi}(1, y; \sigma^*) = 0 & \text{for } 0 \leqslant y \leqslant 1/2, \\ \bar{\phi}(X, 0; \sigma^*) = 0, & \bar{\phi}(X, 1/2; \sigma^*) = 0 & \text{for } 0 \leqslant X \leqslant 1. \end{array}\right\} \quad (3.3)$$

The inlet condition (2.10) becomes

$$\epsilon^{1/2}\left(\phi_{Byy}+\left(\Omega_B\frac{K_0K_{0y}}{2y^2\psi_{0y}^2}-\frac{\psi_{0yyy}}{\psi_{0y}}\right)\phi_B\right)A_X(0;\sigma^*)$$
$$+\epsilon^{3/2}\left(\bar{\phi}_{yyX}(0,y;\sigma^*)+\left(\Omega_B\frac{K_0K_{0y}}{2y^2\psi_{0y}^2}-\frac{\psi_{0yyy}}{\psi_{0y}}\right)\bar{\phi}_X(0,y;\sigma^*)\right)$$
$$+\epsilon^{3/2}\left(\frac{\phi_B}{2y}A_{XXX}(0;\sigma*)+\kappa_\omega\frac{K_0K_{0y}}{2y^2\psi_{0y}^2}\phi_BA_X(0;\sigma^*)\right)+O(\epsilon^2)=0. \tag{3.4}$$

From (3.2), the leading-order term $O(\epsilon)$ in (3.4) vanishes. At $O(\epsilon^{3/2})$, (3.4) becomes

$$\bar{\phi}_{yyX}(0,y;\sigma^*)+\left(\Omega_B\frac{K_0K_{0y}}{2y^2\psi_{0y}^2}-\frac{\psi_{0yyy}}{\psi_{0y}}\right)\bar{\phi}_X(0,y;\sigma^*)$$
$$+\frac{\phi_B}{2y}A_{XXX}(0;\sigma^*)+\kappa_\omega\frac{K_0K_{0y}}{2y^2\psi_{0y}^2}\phi_BA_X(0;\sigma^*)=0. \tag{3.5}$$

We analyse now the linear stability equation (2.8). Substituting (3.1) into (2.8) gives

$$\epsilon\left(\phi_{Byy}+\left(\Omega_B\frac{K_0K_{0y}}{2y^2\psi_{0y}^2}-\frac{\psi_{0yyy}}{\psi_{0y}}\right)\phi_B\right)A_{XX}+\epsilon^2\left(\bar{\phi}_{XXyy}+\left(\Omega_B\frac{K_0K_{0y}}{2y^2\psi_{0y}^2}-\frac{\psi_{0yyy}}{\psi_{0y}}\right)\bar{\phi}_{XX}\right)$$
$$+\epsilon^2\left(\frac{\phi_B}{2y}A_{XXXX}+\kappa_\omega\frac{K_0K_{0y}}{2y^2\psi_{0y}^2}\phi_BA_{XX}+\sigma^*\left(\frac{2}{\psi_{0y}}\phi_{Byy}-\frac{\psi_{0yyy}}{\psi_{0y}^2}\phi_B\right)A_X\right)$$
$$+O(\epsilon^3)=0. \tag{3.6}$$

From (3.2), the leading-order term $O(\epsilon)$ vanishes. At $O(\epsilon^2)$, and using (3.2) for expressing ϕ_{Byy} in terms of ϕ_B, (3.6) becomes

$$\bar{\phi}_{XXyy}+\left(\Omega_B\frac{K_0K_{0y}}{2y^2\psi_{0y}^2}-\frac{\psi_{0yyy}}{\psi_{0y}}\right)\bar{\phi}_{XX}+\frac{\phi_B}{2y}A_{XXXX}+\kappa_\omega\frac{K_0K_{0y}}{2y^2\psi_{0y}^2}\phi_BA_{XX}$$
$$-\sigma^*\left(\Omega_B\frac{K_0K_{0y}}{y^2\psi_{0y}^3}-\frac{\psi_{0yyy}}{\psi_{0y}^2}\right)\phi_BA_X=0. \tag{3.7}$$

Multiplying (3.7) by $\phi_B(y)$, integrating over the domain $0\leqslant y\leqslant 1/2$, integrating the term related to $\bar{\phi}$ by parts and using the boundary conditions (3.3) gives the following solvability condition:

$$\delta A_{XXXX}+\kappa_\omega N_2A_{XX}-\sigma^*N_sA_X=0, \tag{3.8}$$

where

$$\left.\begin{aligned}\delta&=\int_0^{1/2}\frac{\phi_B^2}{2y}\,\mathrm{d}y,\\ N_2&=\int_0^{1/2}\frac{K_0K_{0y}}{2y^2\psi_{0y}^2}\phi_B^2\,\mathrm{d}y,\\ N_s&=\int_0^{1/2}\left(\Omega_B\frac{K_0K_{0y}}{y^2\psi_{0y}^3}-\frac{\psi_{0yyy}}{\psi_{0y}^2}\right)\phi_B^2\,\mathrm{d}y.\end{aligned}\right\} \tag{3.9}$$

Integrating (3.8) with respect to X gives

$$\delta(A_{XXX} - A_{XXX}(0)) + \kappa_\omega N_2(A_X - A_X(0)) - \sigma^* N_s(A - A(0)) = 0. \tag{3.10}$$

In addition, multiplying (3.5) by $\phi_B(y)$, integrating over the domain $0 \leqslant y \leqslant 1/2$, integrating the term related to $\bar{\phi}_{yy}$ by parts, using (3.2) and the boundary conditions (3.3), and using coefficients (3.9) gives the following inlet condition:

$$\delta A_{XXX}(0) + \kappa_\omega N_2 A_X(0) = 0. \tag{3.11}$$

From condition (3.11), (3.10) results in the model eigenvalue problem for the solution of the mode growth rate σ^* and the mode axial shape function $A(X;\sigma^*)$:

$$\sigma^* \tau A = A_{XXX} + \kappa_\omega \beta A_X, \tag{3.12}$$

with inlet conditions $A(0;\sigma^*) = 0$, $A_{XX}(0;\sigma^*) = 0$ and either $A_X(1;\sigma^*) = 0$ or $A(1;\sigma^*) = 0$ at the outlet. Here, we define $\tau = N_s/\delta$ and $\beta = N_2/\delta$. The right-hand side of (3.12) represents the growth rate of the disturbance. The term related to A_X constitutes the mode shape as swirl is changed around Ω_B whereas the term A_{XXX} dictates the spread of the mode shape along the pipe. A rescaling parameter of the linear problem is assumed in the form of $A_X(0;\sigma^*) = 1$.

3.2. *Analysis of the model linear stability problem*

We first identify the neutral critical states according to (3.12) when $\sigma^* = 0$. The neutral mode solutions of (3.12) that satisfy the inlet conditions and the first outlet condition $A_X(1;\sigma^*) = 0$ are $A = \sin((2n-1)\pi X/2)$ (with n being a positive integer) and $\kappa_{\omega,n} = (2n-1)^2\pi^2/(4\beta)$. Then, from the definitions of ϵ and κ_ω, the critical swirls are $\Omega_n = \Omega_B + (2n-1)^2\pi^2/(4\beta L^2)$, i.e. $\omega_1^2 = \Omega_1 = \Omega_B + \pi^2/(4\beta L^2)$, $\omega_2^2 = \Omega_2 = \Omega_B + 9\pi^2/(4\beta L^2)$, and so on. Similarly, the neutral mode solutions of (3.12) that satisfy the inlet conditions and the second outlet condition $A(1;\sigma^*) = 0$ are $A = \sin(n\pi X)$ (here again n is a positive integer) and $\kappa_{\omega,n} = n^2\pi^2/\beta$. Then, the critical swirls are $\Omega_n = \Omega_B + n^2\pi^2/(\beta L^2)$, i.e. $\omega_1^2 = \Omega_1 = \Omega_B + \pi^2/(\beta L^2)$, $\omega_2^2 = \Omega_2 = \Omega_B + 4\pi^2/(\beta L^2)$, and so on.

Integrating (3.12) with respect to X and using the inlet conditions for A gives

$$\sigma^* \tau \int_0^X A(X';\sigma)\,\mathrm{d}X' = A_{XX} + \kappa_\omega \beta A. \tag{3.13}$$

Multiplying (3.13) by A, integrating with respect to X from $X = 0$ to $X = 1$, and using the boundary conditions for A and the relationships $\int_0^1 A(\int_0^X A(X';\sigma^*)\,\mathrm{d}X')\,\mathrm{d}X = \frac{1}{2}(\int_0^1 A\,\mathrm{d}X)^2$ and $\int_0^1 AA_{XX}\,\mathrm{d}X = -\int_0^1 (A_X)^2\,\mathrm{d}X$ results in

$$\frac{1}{2}\sigma^*\tau\left(\int_0^1 A\,\mathrm{d}X\right)^2 = -\int_0^1 (A_X)^2\,\mathrm{d}X + \kappa_\omega\beta\left(\int_0^1 A^2\,\mathrm{d}X\right). \tag{3.14}$$

Similarly, multiplying (3.12) by A, integrating with respect to X from $X = 0$ to $X = 1$ and using the boundary conditions for A and the relationships $\int_0^1 AA_{XXX}\,\mathrm{d}X = A_{XX}(1;\sigma^*)A(1;\sigma^*) + \frac{1}{2}(A_X^2(0;\sigma^*) - A_X^2(1;\sigma^*))$ and $\int_0^1 AA_X\,\mathrm{d}X = \frac{1}{2}A^2(1;\sigma^*)$ results in

$$\sigma^*\tau\left(\int_0^1 A^2\,\mathrm{d}X\right) = A_{XX}(1;\sigma^*)A(1;\sigma^*) + \frac{1}{2}\left(A_X^2(0;\sigma^*) - A_X^2(1;\sigma^*)\right) + \frac{1}{2}\kappa_\omega\beta A^2(1;\sigma^*). \tag{3.15}$$

We now use (3.12), (3.14) and (3.15) to show for the two suggested outlet conditions the change of vortex stability at the respective critical swirl Ω_1 and to describe the related deviations in mode shape as swirl is varied around Ω_1. For the case with outlet condition $A_X(1;\sigma^*)=0$, we assume that the mode shape at swirl levels around $\Omega_1=\Omega_B+\pi^2/(4\beta L^2)$ is given by $A=\sin(\pi X/2)+O(\epsilon_2)$ where $0\leqslant\epsilon_2\ll 1$. Substituting this in (3.14) gives at the leading order $O(1)$,

$$\sigma^*=\frac{\pi^2\beta}{4\tau}\left(\kappa_\omega-\frac{\pi^2}{4\beta}\right)\quad\text{or}\quad\sigma=\frac{\pi^2 N_2}{4N_s L}(\Omega-\Omega_1). \tag{3.16}$$

Here we used $\sigma=\sigma^*\epsilon^{3/2}$, $\epsilon=1/L^2$, $\kappa_\omega\epsilon=\Omega-\Omega_B$, and the definitions in (3.9). The result (3.16) proves the change of the vortex stability around Ω_1, i.e. the perturbation's mode is asymptotically stable ($\sigma<0$) when $\omega<\omega_1$ and unstable ($\sigma>0$) when $\omega>\omega_1$. This again establishes the WR instability, but here for a sufficiently long pipe. Moreover, from (3.12) we find that $\sigma^*\tau A(1;\sigma^*)=A_{XXX}(1;\sigma^*)$. Therefore, as swirl changes from below ω_1 to above ω_1 and σ^* from negative to positive values, $A_{XXX}(1;\sigma^*)$ also changes from negative to positive values. As ω further increases and A_{XXX} becomes sufficiently positive, A_{XX} also increases from negative values to zero and positive values. This shows that the natural mode shape deforms as ω changes around ω_1. From a dynamical point of view, when $\omega<\omega_1$ (in the supercritical region), perturbations are convected downstream towards the outlet and stabilize on a monotonically increasing mode shape with a maximum point at $X=1$ that is the slowest decaying perturbation. On the other hand, when ω increases sufficiently above ω_1 (in the subcritical region), perturbations can move upstream towards the inlet and stabilize on the fastest-growing mode shape with a local minimum point at $X=1$ and a maximum point that moves upstream with the increase of swirl, ahead of $X=1$. These changes in the dominant natural mode shape are demonstrated in the numerical examples in § 4. They affect the production of the perturbation's kinetic energy inside the domain as well as its transfer at the boundaries.

For the case with outlet condition $A(1;\sigma^*)=0$, we assume that the mode shape at swirl levels around $\Omega_1=\Omega_B+\pi^2/(\beta L^2)$ is given by $A=\sin(\pi X)+O(\epsilon_2)$, where again $0\leqslant\epsilon_2\ll 1$. Substituting this in (3.14) gives at the leading order $O(1)$,

$$\sigma^*=\frac{\pi^2\beta}{4\tau}\left(\kappa_\omega-\frac{\pi^2}{\beta}\right)\quad\text{or}\quad\sigma=\frac{\pi^2 N_2}{4N_s L}(\Omega-\Omega_1). \tag{3.17}$$

The result (3.17) proves the change of the vortex stability around Ω_1 for the second outlet condition as well, i.e. the perturbation's mode is asymptotically stable ($\sigma<0$) when $\omega<\omega_1$ and unstable ($\sigma>0$) when $\omega>\omega_1$. This extends the WR instability to the case of a vortex flow in a sufficiently long pipe with a fixed flux at the outlet. Moreover, from (3.15) we find that in this case $\sigma^*\tau(\int_0^1 A^2\,\mathrm{d}X)=\frac{1}{2}(A_X^2(0;\sigma^*)-A_X^2(1;\sigma^*))$. Therefore, as swirl changes from below ω_1 to above ω_1 and σ^* changes from negative to positive values, $A_X^2(0;\sigma^*)-A_X^2(1;\sigma^*)$ also changes from negative to positive values. Again, from a dynamical point of view, when $\omega<\omega_1$ (in the supercritical region), perturbations are convected downstream towards the outlet and the mode shape deviates from the symmetric critical mode about $X=1/2$. It stabilizes on the slowest-decaying mode that is asymmetric about $X=1/2$ and exhibits $A_X^2(0;\sigma^*)<A_X^2(1;\sigma^*)$ and a maximum point location that moves downstream of $X=1/2$ with decrease of swirl. On the other hand, when $\omega>\omega_1$ (in the subcritical region), perturbations can move upstream and stabilize on the fastest-growing mode shape that exhibits $A_X^2(0;\sigma^*)>A_X^2(1;\sigma^*)$ and a maximum point location that moves

upstream of $X = 1/2$ with increase of swirl. These changes in the dominant natural mode shape are also demonstrated in the numerical examples in § 4. They also affect the production of the perturbation's kinetic energy inside the domain as well as its transfer at the boundaries. Also note that the change of growth rate with swirl $\sigma/(\Omega - \Omega_1) = \pi^2 N_2/(4N_s L)$ is the same for the two outlet boundary conditions and depends on the vortex base velocity profiles.

The solution of the eigenvalue problem (3.12) is found numerically by defining $Z_1 = A$, $Z_2 = A_X$, $Z_3 = A_{XX}$ and using the Runge–Kutta fourth-order method in Matlab to solve the system of equations

$$\mathrm{d}Z_1/\mathrm{d}X = Z_2, \quad \mathrm{d}Z_2/\mathrm{d}X = Z_3, \quad \mathrm{d}Z_3/\mathrm{d}X = \sigma^* \tau Z_1 - \kappa_\omega \beta Z_2, \tag{3.18}$$

with inlet conditions $Z_1(0) = 0$, $Z_2(0) = 1$ (a rescaling parameter of the linear problem) and $Z_3(0) = 0$. We use Newton iterations to determine the value of σ^* as a function of κ_ω for which either $Z_1(1) = 0$ or $Z_2(1) = 0$ is satisfied at the outlet. The numerical solution of the problem (3.18) provides the perturbation's leading-order mode shape $\phi(x, y; \sigma) = \phi_B(y) A(X; \sigma^*)$ and its growth rate $\sigma = \sigma^* \epsilon^{3/2}$. The mode shape is extremely important for computing the perturbation's kinetic energy production at the pipe boundaries and inside the domain. In the next section, we describe solutions of the linear stability problem for representative and physically relevant vortices such as the Lamb–Oseen and Q vortices in a long pipe, at a range of swirl levels around the vortex Benjamin's critical swirl Ω_B, and for the two relevant outlet conditions mentioned above. The results will be used in § 6 together with the Reynolds–Orr equation (developed in § 5) to compute the perturbation's kinetic energy production and explore energy transfer mechanisms in the flow and its relationship to flow change of stability at ω_1.

Note that when the pipe is sufficiently long, the solution of the eigenvalue problem (3.12) can be applied to study the linear stability of vortex flows in a pipe with general circumferential and axial velocity profiles, at a range of swirl levels around Ω_B, and with several outlet conditions. Our numerical experience shows that this new asymptotic approach gives accurate results for pipes with $L \geqslant 6$ when compared to the solutions for the Lamb–Oseen vortex obtained by linear operator theory in Wang, Taylor & Ku Akil (2010). The relative error decreases with pipe length. The present approach significantly simplifies the solution of the linear stability problem (2.8) and (2.9), and generalizes it for wider applications. The simplification is a result of the ability to use, in the case of a long pipe, a leading-order solution in the form of separation of variables. This reveals that in a long pipe the small-disturbance linearized evolution can be decoupled in the axial and radial directions and in time. The radial direction is dominated by Benjamin's eigenmode for an infinitely long pipe. The deviations of the axial mode from the critical shape occur along the pipe and at the boundaries and significantly affect the production of the perturbation's kinetic energy at the various places. These deviations support the change of stability characteristics of the flow as swirl level is varied from below the critical level ω_1 to above the next critical level ω_2.

4. The linear stability of Lamb–Oseen and Q vortices in a finite-length, long, circular pipe

The new linear stability problem (3.12) is applied to the family of Q vortex flows where the non-dimensional velocity profiles, scaled with the characteristic inlet axial

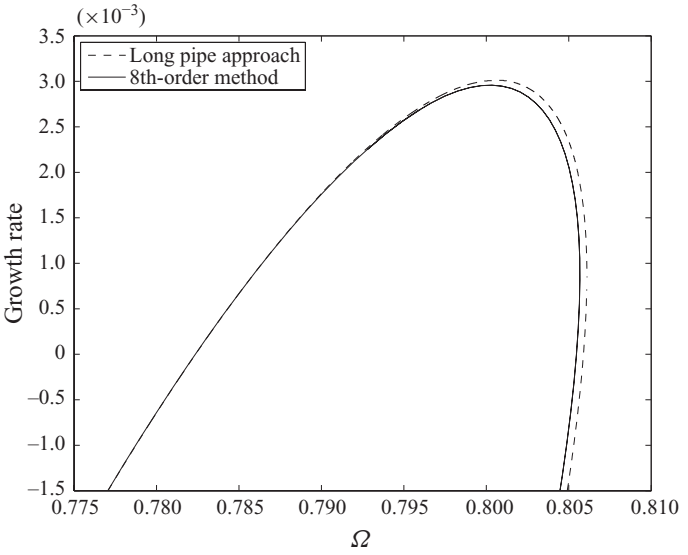

FIGURE 1. The growth rate curves of the Lamb–Oseen vortex with $b=4$, $d=0$, pipe length $L=6$, and the outlet condition $A_X(1;\sigma^*)=0$, computed by using the long-pipe approach, and the eighth-order method based on the linear operator theory of Wang *et al.* (2010).

velocity, are

$$V(y)=\frac{\omega}{\sqrt{2y}}\left(1-\mathrm{e}^{-2b_1y}\right),\quad W(y)=1+d\mathrm{e}^{-2b_2y}. \tag{4.1}$$

Here b_1 is the vortex core-size parameter, where the non-dimensional vortex core radius scaled with the pipe radius is $r_c=1.12/\sqrt{b_1}$, b_2 is the axial velocity shape parameter, and d describes the axial velocity character; $d=0$ is the case of a uniform axial flow (the Lamb–Oseen vortex), $d>0$ is the case of a swirling jet flow, and $-1<d<0$ is the case of a swirling wake flow. These model vortices represent realistic swirling flows in experimental apparatuses such as described in Leibovich's (1984) review paper. In the following examples, we take the representative case where $b_1=b_2=b=4$. Also, a representative pipe of non-dimensional length (scaled with pipe radius) $L=6$ is used, which characterizes the length scale of experimental apparatuses. Then, $\epsilon=1/36$.

We first describe the solutions of (3.12) for the Lamb–Oseen vortex with $b=4$ and $d=0$ and with the first outlet condition $A_X(1;\sigma^*)=0$ and compare the results with the highly accurate eighth-order solution of the linear stability problem (2.8) for the Lamb–Oseen vortex obtained by linear operator theory (Wang *et al.* 2010). Results of the growth rate (σ) as a function of Ω from both solution techniques are shown in figure 1 for a range of swirl levels between $\Omega=0.777$ and $\Omega=0.806$. The figure demonstrates good agreement between the two solution methods for the range of swirls studied. It is noticed that although the present solution shows small deviations from the accurate calculations for $\Omega>0.795$, the two solutions have a similar shape with a fold point at the same growth rate level. The present solution method extends the results of Wang *et al.* (2010) to find the whole branch of growth rates for Ω between the first and second critical swirls. The current method is much simpler than the linear operator method for computing the mode growth rate at swirl levels where $|\Delta\Omega|$ is of the order of ϵ.

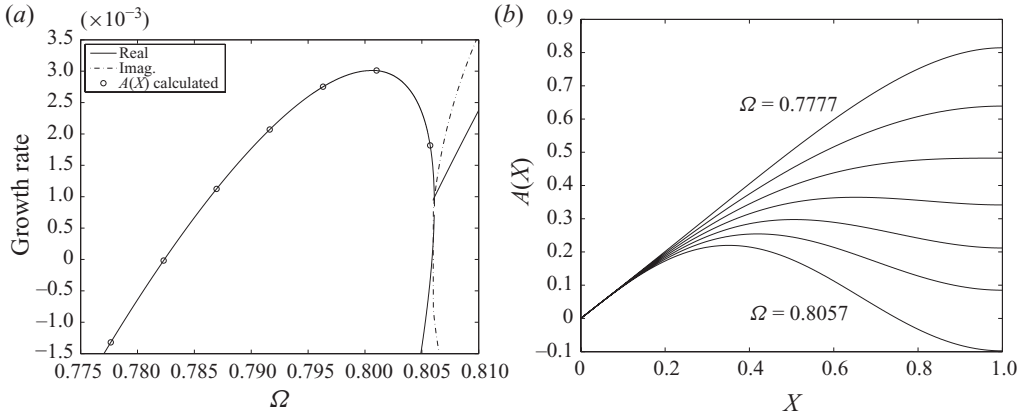

FIGURE 2. (*a*) The growth rate curve of the Lamb–Oseen vortex with $b=4$, $d=0$, pipe length $L=6$ and the outlet condition $A_X(1;\sigma^*)=0$, computed by using the long-pipe approach. (*b*) The corresponding eigenmodes $A(X;\sigma^*)$ for swirl Ω and growth rate σ marked on the growth rate curve.

A remarkable feature of the present method is that the eigenmode can be readily computed in the leading order, which is crucial for further investigation of the energy transfer mechanism between the disturbance and the base flow in a finite-length pipe setting. The computed growth rates and related eigenmodes $A(X;\sigma)$ for several representative points of interest are shown in figure 2 for the swirl between $\Omega=0.7777$ and $\Omega=0.8057$. We can see that the dominant natural eigenmode changes significantly along the pipe axis as Ω is increased from the supercritical region (where $\Omega<\Omega_1$) to the subcritical region (where $\Omega>\Omega_1$). Specifically, the mode's maximum point is at the outlet when $\Omega<\Omega_1$ and it moves upstream with increase of swirl level above Ω_1, as has been predicted in § 3. Also, for same value of the inlet derivative $A_X(0;\sigma^*)=1$, the maximum value of $A(X;\sigma^*)$ decreases and the values near the outlet also decrease and become negative with the increase of swirl level. Essentially, the mode shape shifts with increase of swirl level from the critical mode $\sin(\pi X/2)$ at $\Omega_1=0.7823$ towards the critical mode $\sin(3\pi X/2)$ at $\Omega_2=0.8057$.

The computed growth rates for the Lamb–Oseen vortex with $b=4$ and $d=0$ and with the second outlet condition $A(1,0;\sigma^*)=0$ are shown in figure 3(*a*) for a range of swirls between $\Omega=0.7854$ and $\Omega=0.8269$. The eigenmodes for several representative points of interest in figure 3(*a*) are shown in figure 3(*b*). It can be seen that the first and second critical swirls for this outlet condition increase to $\Omega_1=0.7912$ and $\Omega_2=0.8269$ with respect to those of the first outlet condition. The corresponding neutral eigenmodes, $\sin(\pi X)$ and $\sin(2\pi X)$ respectively, are symmetric about $X=1/2$ (the mid-pipe cross-section). The dominant natural eigenmodes become asymmetric about $X=1/2$ as Ω changes around Ω_1, as predicted in § 3 for this outlet condition. The modes change their shape and maximum points are located towards the outlet and decay in time in the supercritical region where $\Omega<\Omega_1$ (where $\sigma^*<0$). They shift towards the inlet and grow in time in the subcritical region where $\Omega>\Omega_1$ (where $\sigma^*>0$). Also, it can be seen that the radial velocity (related to the X-derivative of the eigenmode) is positive along the inlet, zero near the mid-pipe cross-section and negative along the outlet. This non-periodic mode that changes its shape and stability characteristics is a direct result of the inlet–outlet conditions imposed on the perturbation. Again, essentially the mode shape shifts with the increase of swirl

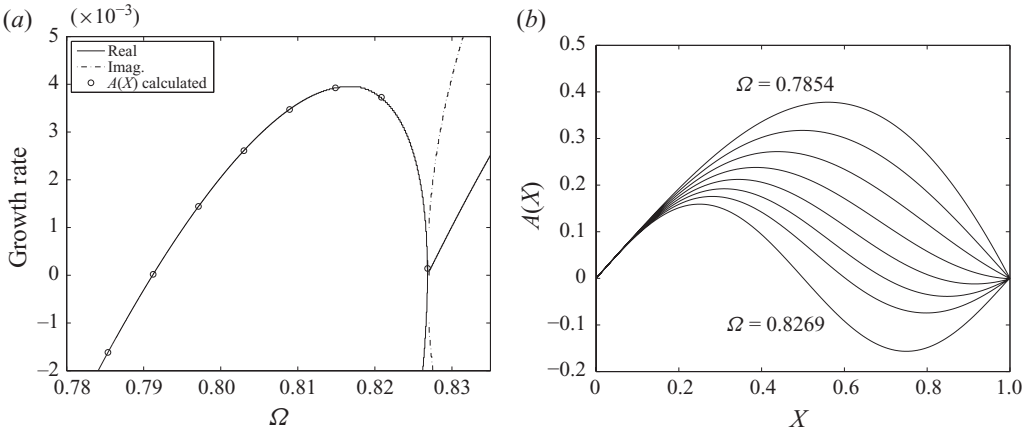

FIGURE 3. (*a*) The growth rate curve of the Lamb–Oseen vortex with $b=4$, $d=0$, pipe length $L=6$ and the outlet condition $A(1;\sigma^*)=0$, computed by using the long-pipe approach. (*b*) The corresponding eigenmodes $A(X;\sigma^*)$ for swirl Ω and growth rate σ marked on the growth rate curve.

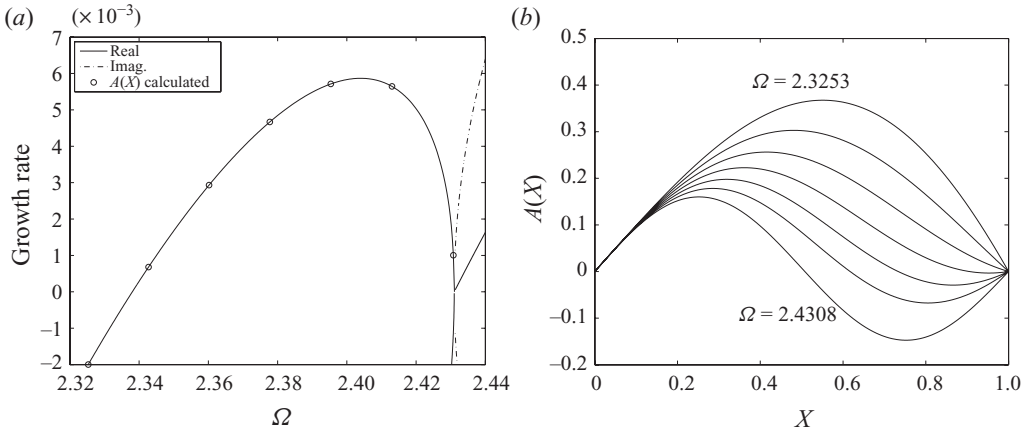

FIGURE 4. (*a*) The growth rate curve of the *Q* vortex with $b=4$, $d=1$, pipe length $L=6$ and the outlet condition $A(1;\sigma^*)=0$, computed using the long-pipe approach. (*b*) The corresponding eigenmodes $A(X;\sigma^*)$ for swirl Ω and growth rate σ marked on the growth rate curve.

from the critical mode $\sin(\pi X)$ at $\omega_1=0.7912$ towards the critical mode $\sin(2\pi X)$ at $\Omega_2=0.8269$.

The computed growth rates for a swirling jet with $b=4$, $d=1$ and with the outlet condition $A(1;\sigma^*)=0$ are shown in figure 4(*a*) for a range of swirls between $\Omega=2.3253$ and $\Omega=2.4308$. The corresponding eigenmodes are shown in figure 4(*b*). The jet axial flow increases the values of the critical levels to $\Omega_1=2.338$ and $\Omega_2=2.4308$, with increased values of growth rates with respect to the Lamb–Oseen vortex. This is a direct result of the increase in the base flow axial velocity at and around the vortex axis. The dominant natural eigenmodes exhibit behaviour similar to the corresponding case described in figure 3(*b*).

The computed growth rates for a swirling wake with $b=4$ and $d=-0.5$ and with the outlet condition $A(1;\sigma^*)=0$ are shown in figure 5(*a*) for a range of swirls between

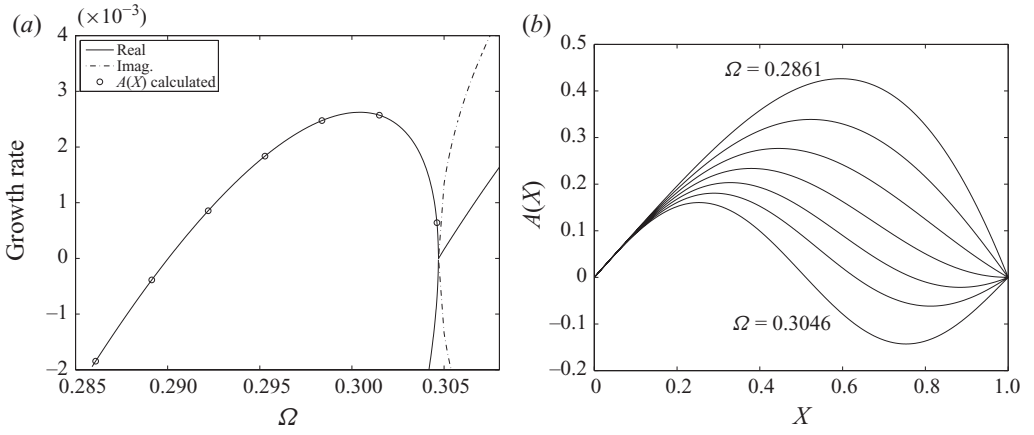

FIGURE 5. (*a*) The growth rate curve of the Q vortex with $b=4$, $d=-0.5$, pipe length $L=6$ and outlet condition $A(1;\sigma^*)=0$, computed by using the long-pipe approach. (*b*) The corresponding eigenmodes $A(X;\sigma^*)$ for swirl Ω and growth rate σ marked on the growth rate curve.

$\Omega=0.2861$ and $\Omega=0.3046$. The corresponding eigenmodes are shown in figure 5(*b*). The wake axial flow decreases the values of the critical levels to $\Omega_1=0.290$ and $\Omega_2=0.304$, with decreased values of growth rates with respect to the Lamb–Oseen vortex. This is a direct result of the decrease in the base flow axial velocity at and around the vortex axis. The dominant natural eigenmodes also exhibit behaviour similar to the corresponding case described in figure 3(*b*).

5. The Reynolds–Orr equation for a swirling flow in a straight finite-length pipe

We now consider a general steady, axisymmetric, non-columnar base flow with velocity components $u=U(x,r)$, $v=V(x,r)$, $w=W(x,r)$ and pressure field $p=P(x,r)$ (the base flow here may not be columnar). Let $u_1=u(x,r,t)-U(x,r)$, $v_1=v(x,r,t)-V(x,r)$, $w_1=w(x,r,t)-W(x,r)$ be the radial, circumferential and axial velocity disturbances from the base flow velocities, respectively, and $p_1=p(x,r,t)-P(x,r)$ be the pressure disturbance. The energy transfer between the disturbances and the base flow can be analysed by the Reynolds–Orr equation. Let $E(t)$ be the specific integrated kinetic energy of the disturbance contained in the finite-length pipe:

$$E(t)=\pi\int_0^L\int_0^1\left(u_1^2+v_1^2+w_1^2\right)r\,\mathrm{d}r\,\mathrm{d}x. \tag{5.1}$$

For an axisymmetric base flow with velocity components (U,V,W), the Reynolds–Orr equation (see, for example, the recent monograph by Wu *et al.* 2006) relates the rate of change in time of the specific integrated kinetic energy of the disturbance $\mathrm{d}E(t)/\mathrm{d}t$ to various 'source' terms, i.e.

$$\frac{\mathrm{d}E(t)}{\mathrm{d}t}=-2\pi\left(\int_0^L\int_0^1(u_1,v_1,w_1)\boldsymbol{B}(u_1,v_1,w_1)^{\mathrm{T}}r\,\mathrm{d}r\,\mathrm{d}x+\int_0^1\left[w_1p_1\right]_{x=0}^{x=L}r\,\mathrm{d}r+\frac{1}{2}\int_0^1\left[W\left(u_1^2+v_1^2+w_1^2\right)\right]_{x=0}^{x=L}r\,\mathrm{d}r\right). \tag{5.2}$$

Here $\boldsymbol{B}$ is the symmetric strain-rate tensor of the base flow, defined in cylindrical coordinates by

$$\boldsymbol{B} = \frac{1}{2}\begin{bmatrix} 2U_r & r\left(\dfrac{V}{r}\right)_r & W_r + U_x \\ r\left(\dfrac{V}{r}\right)_r & \dfrac{2U}{r} & V_x \\ W_r + U_x & V_x & 2W_x \end{bmatrix}. \tag{5.3}$$

The source terms include the production of E inside the flow domain (the first integral on the right-hand side of (5.2)), the production of E caused by the work of the pressure perturbations at the pipe inlet and outlet (the second integral), and the production of E resulting from the convection of E by the axial velocity W at the inlet and outlet (the third integral).

It should be noted that the boundary terms vanish when periodic boundary conditions are applied at the pipe inlet and outlet. Then, for a general vortex flow, the rate of change of the perturbation's kinetic energy is determined only by the production of E inside the flow domain.

For a base columnar swirling flow with $U = 0$, $V = \omega v_0(y)$ and $W = w_0(y)$ (for example, the Q vortex), we have

$$\frac{\mathrm{d}E(t)}{\mathrm{d}t} = -2\pi\left(\omega\int_0^L\int_0^{1/2}\left(K_{0y} - \frac{K_0}{y}\right)u_1 v_1\,\mathrm{d}y\,\mathrm{d}x + \int_0^L\int_0^{1/2}\sqrt{2y}\,w_{0y}u_1 w_1\,\mathrm{d}y\,\mathrm{d}x + \int_0^{1/2}\left[w_1 p_1\right]_{x=0}^{x=L}\mathrm{d}y + \frac{1}{2}\int_0^{1/2} w_0(y)\left[u_1^2 + v_1^2 + w_1^2\right]_{x=0}^{x=L}\mathrm{d}y\right). \tag{5.4}$$

In this case, the production of the perturbation's kinetic energy inside the flow domain is built up of two integrals, one related to the product $u_1 v_1$ and is modulated by the profile of base flow strain rate $(K_{0y} - K_0/y)$, and the second related to the product $u_1 w_1$ and is modulated by the axial velocity profile of the base flow strain rate w_{0y}. For a typical swirling jet flow, $w_{0y} < 0$ for $0 \leqslant y \leqslant 1/2$, and this promotes exchange of energy inside the domain. On the other hand, for a typical swirling wake flow, $w_{0y} > 0$ for $0 \leqslant y \leqslant 1/2$, which suppresses exchange of energy inside the domain. For a columnar swirling base flow with a uniform axial speed $U = 0$, $V = \omega v_0(y)$, $w_0(y) = 1$, the production of the perturbation's kinetic energy inside the flow domain simplifies to only one term.

We note here that for a base columnar flow with a uniform axial speed and imposed periodic inlet–outlet conditions, the second and third terms in (5.2) related to the boundary terms vanish. Then, the rate of change of E in time is governed only by the production term inside the flow domain. Furthermore, for the solid-body rotating flow where $K_0 = 2y$, the strain rate vanishes for all $0 \leqslant y \leqslant 1/2$ and, as a result, the integrand on the right-hand side of (5.4) also vanishes. This establishes $\mathrm{d}E(t)/\mathrm{d}t = 0$, i.e. the conservation of the kinetic energy of the disturbance for the solid-body rotation, thereby making it a waveguide; see Drazin (2002).

In addition, for the case of the solid-body rotation with the present boundary conditions (2.9), again the integral over the flow domain on the right-hand side of (5.4) vanishes. Then, no perturbation kinetic energy is produced inside the domain and it is inactive in determining the flow stability (the domain acts as a waveguide). The terms that involve the boundaries in (5.4) do not vanish and energy transfer at the boundaries occurs to generate the change of stability as swirl ratio is increased

across the critical swirl for solid-body rotation. This recovers the result found by Gallaire & Chomaz (2004).

It should be emphasized that solid-body rotation is the only strain-free vortex flow. For a general vortex flow, for example the Lamb–Oseen vortex, one finds that

$$K_{0y} - \frac{K_0}{y} = 2b\,\mathrm{e}^{-2by} - \frac{1-\mathrm{e}^{-2by}}{y}, \tag{5.5}$$

which is negative in the whole domain $0 < y \leqslant 1/2$.

For the present boundary conditions (2.9) with a fixed flux at the outlet, we have $w_1(0, y, t) = w_1(L, y, t) = 0$. Then, one finds that

$$\frac{\mathrm{d}E(t)}{\mathrm{d}t} = 2\pi\left(\omega\int_0^L\int_0^{1/2}\left(\frac{1-\mathrm{e}^{-2by}}{y} - 2b\,\mathrm{e}^{-2by}\right)u_1v_1\,\mathrm{d}y\,\mathrm{d}x + \frac{1}{2}\int_0^{1/2}\left[u_1^2+v_1^2\right]_{x=L}^{x=0}\mathrm{d}y\right). \tag{5.6}$$

The advantage of this type of a boundary condition is that the second term in (5.2) related to the work of the pressure perturbation becomes inactive. Equation (5.6) clearly establishes that for the Lamb–Oseen vortex, the production of the specific integrated kinetic energy of the disturbance inside of the domain is active (not zero) and interacts with the production of energy from the boundaries. This result shows that solid-body rotation is only a special case of vortex flows where the production of energy inside the domain is inactive. It can be seen that a general vortex flow has richer dynamics than the solid-body rotation. For general vortex flows, the perturbation's kinetic energy production (or loss) inside the domain and at the boundaries interact with each other and affect the stability characteristics of the flow.

For further analysis, we rewrite (5.4) in the form

$$\frac{\mathrm{d}E(t)}{\mathrm{d}t} = 2\pi(E_{uv} + E_{uw} + E_{uu_{outlet}} - E_{uu_{inlet}} + E_{vv_{outlet}} + E_{ww_{outlet}} + E_{wp_{outlet}}), \tag{5.7}$$

where

$$\left.\begin{aligned}
E_{uv} &= -\omega\int_0^L\int_0^{1/2}\left(K_{0y} - \frac{K_0}{y}\right)u_1v_1\,\mathrm{d}y\,\mathrm{d}x,\\
E_{uw} &= -\int_0^L\int_0^{1/2}\sqrt{2y}w_{0y}u_1w_1\,\mathrm{d}y\,\mathrm{d}x,\\
E_{uu_{inlet}} &= -\frac{1}{2}\int_0^{1/2}w_0(y)u_1^2(0, y, t)\,\mathrm{d}y,\\
E_{uu_{outlet}} &= -\frac{1}{2}\int_0^{1/2}w_0(y)u_1^2(L, y, t)\,\mathrm{d}y,\\
E_{vv_{outlet}} &= -\frac{1}{2}\int_0^{1/2}w_0(y)v_1^2(L, y, t)\,\mathrm{d}y,\\
E_{ww_{outlet}} &= -\frac{1}{2}\int_0^{1/2}w_0(y)w_1^2(L, y, t)\,\mathrm{d}y,\\
E_{wp_{outlet}} &= -\int_0^{1/2}w_1(L, y, t)p_1(L, y, t)\,\mathrm{d}y.
\end{aligned}\right\} \tag{5.8}$$

Note that according to the present inlet conditions $v_1(0, y, t) = w_1(0, y, t) = 0$ and, therefore,

$$\left.\begin{aligned} E_{vv_{inlet}} &= -\frac{1}{2}\int_0^{1/2} w_0(y) v_1^2(0, y, t)\,\mathrm{d}y = 0, \\ E_{ww_{inlet}} &= -\frac{1}{2}\int_0^{1/2} w_0(y) w_1^2(0, y, t)\,\mathrm{d}y = 0, \\ E_{wp_{inlet}} &= -\int_0^{1/2} w_1(0, y, t) p_1(0, y, t)\,\mathrm{d}y = 0. \end{aligned}\right\} \tag{5.9}$$

Note that the Reynolds–Orr equation on its own, without a detailed solution of the disturbance field and evolution, does not lead to a sharp estimate of the energy transfer for general swirling flows and to a conclusion about flow stability. However, using the computed disturbance field, a precise estimate of the energy transfer, including where and how the base flow's kinetic energy is transferred to the disturbance or vice versa, can be obtained by applying the Reynolds–Orr equation. This computation is demonstrated in the next section for a general vortex flow at swirl levels around the critical swirl ω_1, where the base flow changes its stability according to the WR instability. Also, specific discussions on the nature of the Lamb–Oseen and the Q vortices are given.

6. Perturbation's kinetic energy transfer mechanism in a long pipe

6.1. *Asymptotic form of the Reynolds–Orr equation for a swirling flow in a long pipe*

We develop an asymptotic form of the Reynolds–Orr equation for a base columnar swirling flow in a straight long pipe. We use the asymptotic solution (3.1) of the stability problem for the dominant natural mode. The detailed derivations of the various terms involved in this section are presented in Appendix B.

Using the perturbation's form (2.4), the assumed mode shape (2.7) and the asymptotic solution (3.1) for a long pipe, we find from § B.1 that the radial, axial and circumferential velocity perturbations may be given by

$$\left.\begin{aligned} u_1(x, y, t) &= \epsilon_1 \bar{u}_1(X, y; \sigma^*)\,\mathrm{e}^{\sigma^* t^*} + \cdots, \\ w_1(x, y, t) &= \epsilon_1 \bar{w}_1(X, y; \sigma^*)\,\mathrm{e}^{\sigma^* t^*} + \cdots, \\ v_1(x, y, t) &= \epsilon_1 \bar{v}_1(X, y; \sigma^*)\,\mathrm{e}^{\sigma^* t^*} + \cdots, \end{aligned}\right\} \tag{6.1}$$

respectively, where $t^* = \epsilon^{3/2} t$. Also,

$$\left.\begin{aligned} \bar{u}_1(X, y; \sigma^*) &= -\frac{1}{\sqrt{2y}}(\epsilon^{1/2}\phi_B(y) A_X + \epsilon^{3/2}\bar{\phi}_X) + O(\epsilon^{5/2}), \\ \bar{w}_1(X, y; \sigma^*) &= \phi_{B_y}(y) A + \epsilon\bar{\phi}_y + O(\epsilon^2), \\ \bar{v}_1(X, y; \sigma^*) &= \frac{\sqrt{\Omega_B} K_{0y}}{\sqrt{2y}\psi_{0y}}\phi_B A + \epsilon\left[\frac{\sqrt{\Omega_B} K_{0y}}{\sqrt{2y}\psi_{0y}}\phi_B \right. \\ &\quad \times \left(\frac{\kappa_\omega}{2\Omega_B} A - \frac{\sigma^*}{\psi_{0y}}\int_0^X A(X'; \sigma^*)\,\mathrm{d}X'\right) \\ &\quad \left. + \frac{\sqrt{\Omega_B} K_{0y}}{\sqrt{2y}\psi_{0y}}\bar{\phi}\right] + O(\epsilon^2). \end{aligned}\right\} \tag{6.2}$$

From (5.8), (6.1) and (6.2) we find that

$$\left.\begin{aligned}
E_{uv} &= \epsilon_1^2\,\mathrm{e}^{2\sigma^* t^*}\left(\bar{E}^0_{uv} + \epsilon\bar{E}^\epsilon_{uv} + O(\epsilon^2)\right) + \cdots,\\
E_{uw} &= \epsilon_1^2\,\mathrm{e}^{2\sigma^* t^*}\left(\bar{E}^0_{uw} + \epsilon\bar{E}^\epsilon_{uw} + O(\epsilon^2)\right) + \cdots,\\
E_{uu_{inlet}} &= \epsilon_1^2\,\mathrm{e}^{2\sigma^* t^*}\left(\bar{E}^0_{uu_{inlet}} + \epsilon\bar{E}^\epsilon_{uu_{inlet}} + O(\epsilon^2)\right) + \cdots,\\
E_{uu_{outlet}} &= \epsilon_1^2\,\mathrm{e}^{2\sigma^* t^*}\left(\bar{E}^0_{uu_{outlet}} + \epsilon\bar{E}^\epsilon_{uu_{outlet}} + O(\epsilon^2)\right) + \cdots,\\
E_{vv_{outlet}} &= \epsilon_1^2\,\mathrm{e}^{2\sigma^* t^*}\left(\bar{E}^0_{vv_{outlet}} + \epsilon\bar{E}^\epsilon_{vv_{outlet}} + O(\epsilon^2)\right) + \cdots,\\
E_{ww_{outlet}} &= \epsilon_1^2\,\mathrm{e}^{2\sigma^* t^*}\left(\bar{E}^0_{ww_{outlet}} + \epsilon\bar{E}^\epsilon_{ww_{outlet}} + O(\epsilon^2)\right) + \cdots,\\
E_{wp_{outlet}} &= \epsilon_1^2\,\mathrm{e}^{2\sigma^* t^*}\left(\bar{E}^0_{wp_{outlet}} + \epsilon\bar{E}^\epsilon_{wp_{outlet}} + O(\epsilon^2)\right) + \cdots.
\end{aligned}\right\} \tag{6.3}$$

The various terms in (6.3) are derived in § B.2; the leading-order terms are

$$\left.\begin{aligned}
\bar{E}^0_{uv} &= -\tfrac{1}{2}\Omega_B(M_{3a} - M_{3b})A^2(1;\sigma^*),\\
\bar{E}^0_{uw} &= \tfrac{1}{2}J_1 A^2(1;\sigma^*),\\
\bar{E}^0_{uu_{inlet}} &= \bar{E}^0_{uu_{outlet}} = 0,\\
\bar{E}^0_{vv_{outlet}} &= -\tfrac{1}{2}\Omega_B M_{3b}A^2(1;\sigma^*),\\
\bar{E}^0_{ww_{outlet}} &= -\tfrac{1}{2}(\Omega_B M_{3a} + J_1)A^2(1;\sigma^*),\\
\bar{E}^0_{wp_{outlet}} &= \Omega_B M_{3a}A^2(1;\sigma^*),
\end{aligned}\right\} \tag{6.4}$$

and the first-order terms are

$$\left.\begin{aligned}
\bar{E}^\epsilon_{uv} &= -\frac{1}{2}\kappa_\omega(M_{3a} - M_{3b})A^2(1;\sigma^*) + \sigma^*\Omega_B(N_{3a} - N_{3b})\\
&\quad\times\left[A(1;\sigma^*)\int_0^1 A(X';\sigma^*)\,\mathrm{d}X' - \int_0^1 A^2(X';\sigma^*)\,\mathrm{d}X'\right] - \Omega_B(I_1 - I_2)A(1;\sigma^*),\\
\bar{E}^\epsilon_{uw} &= \frac{1}{2}\kappa_\omega M_{3a}A^2(1;\sigma^*) + \frac{1}{2}\delta_W\left[A_X^2(1;\sigma^*) - A_X^2(0;\sigma^*)\right]\\
&\quad-\sigma^*(2\Omega_B N_{3a} + J_2)\left[A(1;\sigma^*)\int_0^1 A(X';\sigma^*)\,\mathrm{d}X' - \int_0^1 A^2(X';\sigma^*)\,\mathrm{d}X'\right]\\
&\quad-\left[\int_0^{1/2}\chi_0\phi_{By}\bar{\phi}(1,y;\sigma^*)\,\mathrm{d}y\right]A(1;\sigma^*),\\
\bar{E}^\epsilon_{uu_{inlet}} &= -\frac{1}{2}\delta_W A_X^2(0;\sigma^*),\\
\bar{E}^\epsilon_{uu_{outlet}} &= -\frac{1}{2}\delta_W A_X^2(1;\sigma^*),\\
\bar{E}^\epsilon_{vv_{outlet}} &= -\frac{1}{2}\kappa_\omega M_{3b}A^2(1;\sigma^*) + \sigma^*\Omega_B N_{3b}A(1;\sigma^*)\int_0^1 A(X';\sigma^*)\,\mathrm{d}X' - \Omega_B I_2 A(1;\sigma^*),\\
\bar{E}^\epsilon_{ww_{outlet}} &= -\Omega_B I_1 A(1;\sigma^*) - \left[\int_0^{1/2}(\chi_0\phi_{By} + \chi_{0y}\phi_B)\bar{\phi}(1,y;\sigma^*)\,\mathrm{d}y\right]A(1;\sigma^*),\\
\bar{E}^\epsilon_{wp_{outlet}} &= \sigma^*(\Omega_B N_{3a} + J_2)A(1;\sigma^*)\int_0^1 A(X';\sigma^*)\,\mathrm{d}X' + 2\Omega_B I_1 A(1;\sigma^*)\\
&\quad+\left[\int_0^{1/2}(2\chi_0\phi_{By} + \chi_{0y}\phi_B)\bar{\phi}(1,y;\sigma^*)\,\mathrm{d}y\right]A(1;\sigma^*).
\end{aligned}\right\} \tag{6.5}$$

Here, we define

$$\left.\begin{aligned} M_{3a} &= \int_0^{1/2} \frac{K_0 K_{0y}}{2y^2\psi_{0y}}\phi_B^2\,\mathrm{d}y, \qquad M_{3b} = \int_0^{1/2} \frac{K_{0y}^2}{2y\psi_{0y}}\phi_B^2\,\mathrm{d}y, \\ N_{3a} &= \int_0^{1/2} \frac{K_0 K_{0y}}{2y^2\psi_{0y}^2}\phi_B^2\,\mathrm{d}y, \qquad N_{3b} = \int_0^{1/2} \frac{K_{0y}^2}{2y\psi_{0y}^2}\phi_B^2\,\mathrm{d}y, \\ I_1 &= \int_0^{1/2} \frac{K_0 K_{0y}}{2y^2\psi_{0y}}\phi_B\bar{\phi}(1,y;\sigma^*)\,\mathrm{d}y, \qquad I_2 = \int_0^{1/2} \frac{K_{0y}^2}{2y\psi_{0y}}\phi_B\bar{\phi}(1,y;\sigma^*)\,\mathrm{d}y, \\ J_1 &= \int_0^{1/2} \chi_{0y}\phi_B^2\,\mathrm{d}y, \qquad J_2 = \int_0^{1/2} \frac{\chi_{0y}}{\psi_{0y}}\phi_B^2\,\mathrm{d}y, \qquad \delta_W = \frac{1}{2}\int_0^{1/2} w_0(y)\frac{\phi_B^2}{2y}\,\mathrm{d}y. \end{aligned}\right\} \tag{6.6}$$

The asymptotic form of the Reynolds–Orr equation (5.7) for a swirling flow in a long pipe results in

$$\frac{\mathrm{d}E(t)}{\mathrm{d}t} = \epsilon_1^2\,\mathrm{e}^{2\sigma^* t^*}\frac{\mathrm{d}E(t)}{\mathrm{d}t}\Big|_{t=0}, \tag{6.7}$$

where

$$\begin{aligned} \frac{\mathrm{d}E(t)}{\mathrm{d}t}\Big|_{t=0} = 2\pi\big[&\big(\bar{E}^0_{uv} + \bar{E}^0_{uw} + \bar{E}^0_{uu_{outlet}} - \bar{E}^0_{uu_{inlet}} + \bar{E}^0_{vv_{outlet}} + \bar{E}^0_{ww_{outlet}} + \bar{E}^0_{wp_{outlet}}\big) \\ &+ \epsilon\big(\bar{E}^\epsilon_{uv} + \bar{E}^\epsilon_{uw} + \bar{E}^\epsilon_{uu_{outlet}} - \bar{E}^\epsilon_{uu_{inlet}} + \bar{E}^\epsilon_{vv_{outlet}} + \bar{E}^\epsilon_{ww_{outlet}} \\ &+ \bar{E}^\epsilon_{wp_{outlet}}\big) + O(\epsilon^2)\big]. \end{aligned} \tag{6.8}$$

6.2. *The perturbation's kinetic energy budget at leading order* $O(1)$

Equations (6.4), (6.7) and (6.8) show the expected result: at order $O(1)$,

$$\bar{E}^0_{uv} + \bar{E}^0_{uw} + \bar{E}^0_{uu_{outlet}} - \bar{E}^0_{uu_{inlet}} + \bar{E}^0_{vv_{outlet}} + \bar{E}^0_{ww_{outlet}} + \bar{E}^0_{wp_{outlet}} = 0, \tag{6.9}$$

i.e. the net perturbation's kinetic energy transfer between the disturbance and base flow vanishes at the leading order.

This result is true for any vortex flow at all swirl levels and for the two possible outlet conditions. Also, note that in the case with a fixed flux outlet condition we have $A(1;\sigma^*) = 0$ and then all the leading-order terms (6.4) are identically zero and (6.9) is identically satisfied. On the other hand, for the case with a columnar outlet state (discussed in WR), $A(1;\sigma^*) \neq 0$. For the Lamb–Oseen or Q vortices, we find that for all b, $K_{0y} = 2b\,\mathrm{e}^{-2by} > 0$ for $0 \leqslant y \leqslant 1/2$ (the vortices are stable according to Rayleigh's criterion) and $K_{0y} - K_0/y < 0$ for $0 < y \leqslant 1/2$ (the base strain rate is negative, see figure 6). Therefore, $M_{3a} > M_{3b} > 0$. As a result, (i) $\bar{E}^0_{uv} < 0$, i.e. the disturbance loses its kinetic energy to the base flow inside the flow domain due to the interaction between the radial velocity perturbation and circumferential velocity perturbation; (ii) $\bar{E}^0_{vv_{outlet}} < 0$ and $\bar{E}^0_{uw} + \bar{E}^0_{ww_{outlet}} < 0$, i.e. representing the convective loss of the disturbance's kinetic energy inside the domain and at the outlet; (iii) $\bar{E}^0_{wp_{outlet}} > 0$, i.e. indicating that $w_1(L,y,t)$ and $p_1(L,y,t)$ are opposite in sign (as expected) and a gain of the disturbance's kinetic energy from the work of the pressure perturbation at the outlet. In summary, at the leading order, for all swirl levels around the critical swirl, the loss of the disturbance's kinetic energy to the base flow inside the domain and the convective loss of the disturbance's kinetic energy inside the domain and at the outlet are

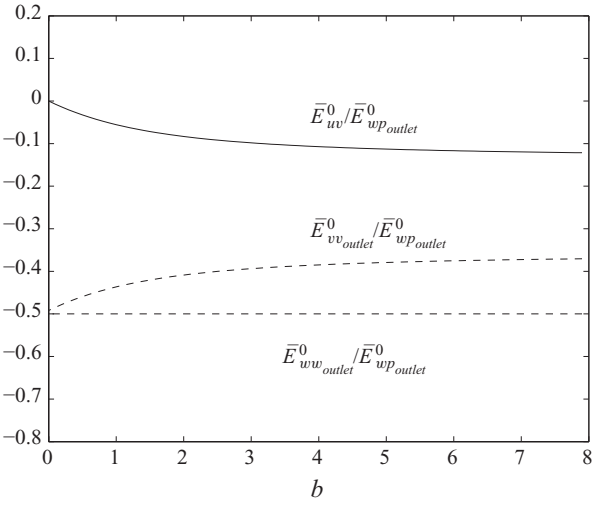

FIGURE 6. $\bar{E}^0_{uv}/\bar{E}^0_{wp_{outlet}}$, $\bar{E}^0_{vv_{outlet}}/\bar{E}^0_{wp_{outlet}}$ and $\bar{E}^0_{ww_{outlet}}/\bar{E}^0_{wp_{outlet}}$ versus the flow parameter b.

balanced by the gain of the disturbance's kinetic energy due to the work of the pressure perturbation at the outlet and there is no net production or loss of the perturbation's kinetic energy.

We define the following ratios of the perturbation's kinetic energy transfer inside the domain and at the outlet divided by the gain of disturbance kinetic energy due to the work of the pressure perturbation at the outlet, i.e.

$$\left.\begin{aligned} R^0_{E,uv} &= \frac{\bar{E}^0_{uv}}{\bar{E}^0_{wp_{outlet}}} = \frac{M_{3b}}{2M_{3a}} - \frac{1}{2}, \\ R^0_{E,uw} &= \frac{\bar{E}^0_{uw}}{\bar{E}^0_{wp_{outlet}}} = \frac{J_1}{2M_{3a}}, \\ R^0_{E,vv} &= \frac{\bar{E}^0_{vv_{outlet}}}{\bar{E}^0_{wp_{outlet}}} = -\frac{M_{3b}}{2M_{3a}}, \\ R^0_{E,ww} &= \frac{\bar{E}^0_{ww_{outlet}}}{\bar{E}^0_{wp_{outlet}}} = -\frac{1}{2}. \end{aligned}\right\} \tag{6.10}$$

We demonstrate these results for the Lamb–Oseen vortex at various values of the core parameter b. Then, $J_1 = 0$ and $\bar{E}^0_{uw} = R^0_{E,uw} = 0$. The values of the leading-order terms $\bar{E}^0_{uv}$, $\bar{E}^0_{vv_{outlet}}$, $\bar{E}^0_{ww_{outlet}}$ and $\bar{E}^0_{wp_{outlet}}$ are computed. The values of $R^0_{E,uv}$, $R^0_{E,vv}$ and $R^0_{E,ww}$ as a function of b in the range (0, 8) are shown in figure 6. It can be seen that $\bar{E}^0_{uv}$ approaches zero as b tends to 0, reflecting the fact that there is no perturbation kinetic energy production (loss) inside the domain for a solid-body rotation. The absolute value of $\bar{E}^0_{uv}$ increases with the increase of b (decrease of vortex core radius) to a level about 12 % of $\bar{E}^0_{wp_{outlet}}$ for $b = 8$. The more slender the vortex core is, the more significant the loss of the disturbance's kinetic energy is to the base flow inside the domain.

6.3. *The perturbation's kinetic energy budget at order* $O(\epsilon)$

Equations (6.5), (6.7) and (6.8) show that at order $O(\epsilon)$,

$$\frac{\mathrm{d}E(t)}{\mathrm{d}t} = \epsilon_1^2 \epsilon\, \mathrm{e}^{2\sigma^* t^*} 2\pi\sigma^* [\Omega_B(N_{3a} + N_{3b}) + J_2] \int_0^1 A^2(X;\sigma^*)\,\mathrm{d}X, \tag{6.11}$$

which is but

$$\frac{\mathrm{d}E(t)}{\mathrm{d}t} = 2\sigma^* \epsilon\, \mathrm{e}^{2\sigma^* t^*} E(0). \tag{6.12}$$

One can also verify this result by a direct substitution of (6.1) and (6.2) into (5.1).

Remark 6.1. The result (6.11) demonstrates the strong coupling of the perturbation's energy production at the boundaries and inside the domain. In fact, (6.11) is derived by the mutual cancellations of the perturbation's energy production terms in the domain and at the boundaries when they are summed in (6.8).

For general vortices such as the Lamb–Oseen or Q vortices $\Omega_B(N_{3a} + N_{3b}) + J_2 > 0$ for all b, and obviously $\epsilon = 1/L^2 > 0$ and $\int_0^1 A^2(X;\sigma^*)\,\mathrm{d}X > 0$. It can be seen that the net perturbation kinetic energy transfer between the disturbance and the base flow is directly related to the growth rate σ^* as a function of the swirl level Ω. We therefore find that there is no production of kinetic energy when $\omega = \omega_1$ (where $\sigma^* = 0$ is a neutral state), there is a decay in time of disturbance kinetic energy when $\omega < \omega_1$ (where $\sigma^* < 0$ are asymptotically stable states) and there is a gain of disturbance kinetic energy when $\omega > \omega_1$ (where $\sigma^* > 0$ are unstable states).

Equations (6.5) shed light on the details of exchange of the perturbation's kinetic energy between the flow domain and the boundaries as the swirl level increases around the critical swirl. Let

$$\left.\begin{aligned} \bar{E}^{\epsilon}_{domain} &= \bar{E}^{\epsilon}_{uv} + \bar{E}^{\epsilon}_{uw}, \\ \bar{E}^{\epsilon}_{boundaries} &= \bar{E}^{\epsilon}_{uu_{inlet}} - \left(\bar{E}^{\epsilon}_{uu_{outlet}} + \bar{E}^{\epsilon}_{vv_{outlet}} + \bar{E}^{\epsilon}_{ww_{outlet}} + \bar{E}^{\epsilon}_{wp_{outlet}}\right). \end{aligned}\right\} \tag{6.13}$$

Here, $\bar{E}^{\epsilon}_{domain}$ is the total production or loss of the perturbation's kinetic energy inside the flow domain at order $O(\epsilon)$ and $\bar{E}^{\epsilon}_{boundaries}$ is the net difference between the inlet and the outlet transfer of the perturbation's kinetic energy at order $O(\epsilon)$. We find from (6.5) that

$$\bar{E}^{\epsilon}_{domain} - \bar{E}^{\epsilon}_{boundaries} = \sigma^* \left[\Omega_B(N_{3a} + N_{3b}) + J_2\right] \int_0^1 A^2(X;\sigma^*)\,\mathrm{d}X. \tag{6.14}$$

Following the previous arguments, this result shows that for general vortices such as the Lamb–Oseen or Q vortices $\bar{E}^{\epsilon}_{domain} = \bar{E}^{\epsilon}_{boundaries}$ at the neutral state $\omega = \omega_1$ (where $\sigma^* = 0$), $\bar{E}^{\epsilon}_{domain} < \bar{E}^{\epsilon}_{boundaries}$ when $\omega < \omega_1$ (where $\sigma^* < 0$) and $\bar{E}^{\epsilon}_{domain} > \bar{E}^{\epsilon}_{boundaries}$ when $\omega > \omega_1$ (where $\sigma^* > 0$).

We conclude that for a general vortex flow and the two possible outlet conditions,

(i) there is a critical balance between the production of the perturbation's kinetic energy inside the domain and at the boundaries at the critical swirl ω_1;

(ii) the asymptotic stability of the base vortex flow at swirl levels below the critical level (in the supercritical swirl region) is related to less production of disturbance kinetic energy inside the domain with respect to the net transfer of kinetic energy at the boundaries; and

(iii) the WR vortex instability at swirl levels above the critical level (in the subcritical swirl region) is related to more production of disturbance kinetic energy inside the domain with respect to the net transfer of kinetic energy at the boundaries.

6.4. *The energy budget at order $O(\epsilon)$ for the outlet condition $w_1(L, y, t) = 0$*

To study the perturbation's kinetic energy production mechanism, we must investigate the separate contributions from the boundaries and the bulk, respectively. We conduct a case study for the specific case where the fixed flux outlet condition $w_1(L, y, t) = 0$ is applied and additional analytical insight can be gained. In this case, $A(1;\sigma^*) = 0$. Then we have from (6.5):

$$\left.\begin{aligned}
&\bar{E}^{\epsilon}_{uv} = -\sigma^* \Omega_B (N_{3a} - N_{3b}) \left[\int_0^1 A^2(X;\sigma^*)\,\mathrm{d}X \right], \\
&\bar{E}^{\epsilon}_{uw} = \frac{1}{2}\delta_W \left[A_X^2(1;\sigma^*) - A_X^2(0;\sigma^*) \right] + \sigma^* (2\Omega_B N_{3a} + J_2) \left[\int_0^1 A^2(X;\sigma^*)\,\mathrm{d}X \right], \\
&\bar{E}^{\epsilon}_{uu_{inlet}} = -\frac{1}{2}\delta_W A_X^2(0;\sigma^*), \quad \bar{E}^{\epsilon}_{uu_{outlet}} = -\frac{1}{2}\delta_W A_X^2(1;\sigma^*), \\
&\bar{E}^{\epsilon}_{vv_{outlet}} = 0, \quad \bar{E}^{\epsilon}_{ww_{outlet}} = 0, \quad \bar{E}^{\epsilon}_{wp_{outlet}} = 0.
\end{aligned}\right\} \tag{6.15}$$

In this case, none of the terms depends on $\bar{\phi}$,

$$\bar{E}^{\epsilon}_{boundaries} = \tfrac{1}{2}\delta_W \left[A_X^2(1;\sigma^*) - A_X^2(0;\sigma^*) \right] \tag{6.16}$$

and (6.14) holds. Using (3.15) and the outlet condition $A(1;\sigma^*) = 0$, we can further simplify $\bar{E}^{\epsilon}_{boundaries}$:

$$\bar{E}^{\epsilon}_{boundaries} = -\sigma^* \delta_W \tau \int_0^1 A^2(X;\sigma^*)\,\mathrm{d}X. \tag{6.17}$$

It can be seen that $\bar{E}^{\epsilon}_{boundaries} > 0$ when $\Omega < \Omega_1$ ($\sigma^* < 0$) and $\bar{E}^{\epsilon}_{boundaries} < 0$ when $\Omega > \Omega_1$ ($\sigma^* > 0$) and is directly related in this case to the deviations of mode shape from symmetry about $X = 1/2$.

Let R^{ϵ}_E denote the ratio of the kinetic energy production inside the domain at order $O(\epsilon)$ over the net kinetic energy transfer at the boundaries at order $O(\epsilon)$, i.e.

$$R^{\epsilon}_E = \frac{\bar{E}^{\epsilon}_{domain}}{\bar{E}^{\epsilon}_{boundaries}}. \tag{6.18}$$

From (6.14) we have

$$R^{\epsilon}_E = 1 + \frac{2\sigma^* \left[\Omega_B (N_{3a} + N_{3b}) + J_2 \right] \displaystyle\int_0^1 A^2(X;\sigma^*)\,\mathrm{d}X}{\delta_W \left[A_X^2(1;\sigma^*) - A_X^2(0;\sigma^*) \right]}, \tag{6.19}$$

and from (6.16) and (6.17) we find that for a general base vortex flow with a fixed flux imposed at the outlet, the ratio R^{ϵ}_E is a characteristic constant property of the flow,

$$R^{\epsilon}_E = 1 - \frac{\Omega_B (N_{3a} + N_{3b}) + J_2}{\delta_W \tau}. \tag{6.20}$$

In addition, using (6.16) and (6.17) in the expression for $\bar{E}^{\epsilon}_{uw}$ in (6.15) gives

$$\bar{E}^{\epsilon}_{uw} = \sigma^* (2\Omega_B N_{3a} + J_2 - \delta(W\tau) \left[\int_0^1 A^2(X;\sigma^*)\,\mathrm{d}X \right]. \tag{6.21}$$

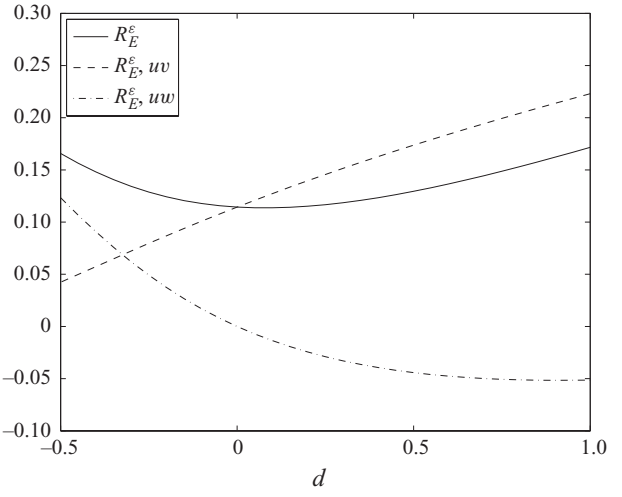

FIGURE 7. The relationship between d and R_E^ϵ, $R_{E,uv}^\epsilon$ and $R_{E,uw}^\epsilon$ for the Q vortex with $b=4$.

Let

$$R_{E,uv}^\epsilon = \frac{\bar{E}_{uv}^\epsilon}{\bar{E}_{boundaries}^\epsilon} \quad \text{and} \quad R_{E,uw}^\epsilon = \frac{\bar{E}_{uw}^\epsilon}{\bar{E}_{boundaries}^\epsilon} \tag{6.22}$$

be the ratios related to the perturbation's kinetic energy inside the domain resulting from uv and uw, respectively. From the expression for $\bar{E}_{uv}^\epsilon$ in (6.15), for $\bar{E}_{uw}^\epsilon$ in (6.21) and for $\bar{E}_{boundaries}^\epsilon$ in (6.17), we also find that for a general base vortex flow with a fixed flux imposed at the outlet, the ratios $R_{E,uv}^\epsilon$ and $R_{E,uw}^\epsilon$ are characteristic constant properties of the flow,

$$\left.\begin{aligned} R_{E,uv}^\epsilon &= \frac{\Omega_B(N_{3a}-N_{3b})}{\delta_W\tau}, \\ R_{E,uw}^\epsilon &= 1-\frac{2\Omega_B N_{3a}+J_2}{\delta_W\tau}. \end{aligned}\right\} \tag{6.23}$$

Figure 7 shows for the Q vortex the calculated values of the base flow properties $\bar{E}_{uw}^\epsilon$, $R_{E,uv}^\epsilon$ and $R_{E,uw}^\epsilon$ as a function of the axial flow parameter d for a fixed vortex core parameter $b=4$. It is found that $\bar{E}_{uw}^\epsilon$ is a monotonically decreasing function of d while $R_{E,uv}^\epsilon$ is a monotonically increasing function of d. The resulting R_E^ϵ decreases from 0.16 for $d=-0.5$ to 0.12 for $d=0.2$ and increases thereafter to 0.165 for $d=1$. Thus, swirling flows with strong wakes ($d=-0.5$) or strong jets ($d=1$) enhance the perturbation's kinetic energy transfer inside the domain.

For the Lamb–Oseen vortex $w_0(y)=1$, $J_2=0$, $\delta_W=\delta$, $\delta_W\tau=N_s=2\Omega_B N_2$ (see (3.9)) and $E_{uw}^\epsilon=R_{E,uw}^\epsilon=0$. Then, the base flow characteristic constants are

$$R_E^\epsilon = R_{E,uv}^\epsilon = \frac{1}{2}-\frac{N_{3b}}{2N_2}. \tag{6.24}$$

Figure 8 shows the calculated relationship between R_E^ϵ and vortex core parameter b. It was found that $R_E^\epsilon>0$ for all b, indicating the opposite energy transfer directions from inside the domain and from the boundary. The magnitude of the ratio R_E^ϵ increases with the increase of b (decrease of core radius) from $R_E^\epsilon=0$ as b tends to zero (the case of a solid-body rotation) to R_E^ϵ of about 14.2 % at $b=50$.

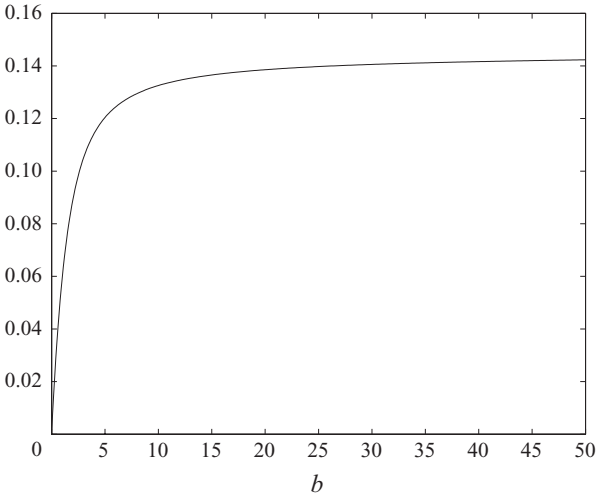

FIGURE 8. R_E^c versus the flow parameter b.

7. Discussion

7.1. *Vortex stability mechanisms*

As is well known, the WR instability is fundamentally different from the classical Rayleigh stability theory. It is therefore important to add to the understanding of this stability (instability) mechanism.

Classical vortex stability theory (Rayleigh 1916) shows that the Lamb–Oseen vortex in an infinitely long, constant-area circular pipe, or, equivalently, in a finite-length, straight, circular pipe with periodic boundary conditions, is neutrally stable to axisymmetric disturbances. To further understand the Rayleigh vortex stability mechanism, it is useful and instructive to examine the recent nonlinear stability theory of Wang (2009). It has been discovered that the Rayleigh criterion is also a necessary and sufficient condition for the nonlinear stability. An upper bound of the disturbance's kinetic energy has been obtained, which is valid for any initial disturbance with a finite amplitude. The nonlinear stability theory of Wang (2009) also offers a new insight into the stability mechanism of swirling flow. A careful examination of the nonlinear stability theory shows that the nonlinear stability relies crucially on two physical facts that hold for an ideal vortex flow:

(*a*) The infinitely long axially uniform vortex flow forms a translation-invariant problem, which, according to the Noether theorem (see, for example, Arnold 1989; Szeri & Holmes 1988), implies the preservation of the axial momentum flux in time. The absence of an axial external force restricts the kinetic energy transfer between the disturbance and the base flow. One notes that in the linear stability theory, the translation-invariant nature is reflected by using the axial normal Fourier mode, where the axial modes are only supporting the disturbance propagation, and the vortex stability is solely determined by the radial modes.

(*b*) Owing to the lack of axial perturbation instability mechanism, the only instability is the centrifugal instability that is set in flow by the kinetic energy released from the azimuthal velocity component to the perturbation. For a base flow that satisfies the Rayleigh criterion, the kinetic energy that can be released from the azimuthal velocity component is bounded and can be estimated by using an Arnold function. The Arnold function gives an estimate of the possible kinetic energy that

can be released from the azimuthal velocity component under the physical constraint that the circulation (Kelvin's circulation theorem) and volumetric flux of the flow are preserved.

On the other hand, for swirling flows in a finite-length, straight, circular pipe under the influence of the physical non-periodic boundary conditions that are studied in this paper, a new kinetic energy transfer mechanism arises. This is because the physical setting at the pipe inlet and outlet exerts an axial force on the flow which effectively changes the axial momentum flux (the flow force, studied in Wang & Rusak 1997*a*) and completely eliminates the basic vortex stability mechanism according to Rayleigh. Therefore, it is not surprising that another type of flow instability that is different from the classical Rayleigh's stability mechanism develops in the flow. This is the WR instability which is related to the instability of the axial modes that fit the linear stability equation and connect between the non-periodic boundary conditions. It should be emphasized that the physical non-periodic boundary conditions serve merely as a kinetic energy transfer agency and the stability is determined by the interaction of the base flow with the axial perturbation in the domain and with the boundary. The stability analysis conducted in WR was the first stability analysis of swirling flow which took into account the axial confinement effect of a finite-length pipe. In this sense, the WR instability which develops at relatively high swirls is but a demonstration of the consequence of the elimination of Rayleigh's stability mechanism due to the axial confinement effect of a finite-length pipe.

It should also be emphasized that the interaction between the small disturbance, base flow and boundary conditions is complicated. The linear stability problem (2.8) and (2.9) shows that the disturbance dynamics involves the wave structure and its propagation in both the radial and axial directions and its interaction with the boundaries. This problem allows an exact analytical solution only for the solid-body rotation flow in a finite-length pipe (Wang & Rusak 1996). For a general base vortex flow such as the Lamb–Oseen and Q vortices, the solution of this stability problem requires a special series solution method (Wang *et al.* 2009) or numerical techniques (Leclaire & Sipp 2010). However, these approaches cannot shed explicit light on the perturbation structure and the energy production from the various components of the flow. Fortunately, in real swirling flow apparatuses, the pipe is sufficiently long compared to its radius such that the long-wave asymptotic approach presented in this paper is valid. Using this approach, we are able to reduce the vortex stability problem to a simpler problem, yet retaining all the essential physics of the flow. The underlying physics governing this reduction, as expressed in (3.1), is that in swirling flows confined in a long straight pipe the axial structure and propagation of the dominant disturbances is much more important than its propagation in the radial direction. This physical insight gained from the asymptotic solution, coupled with the Reynolds–Orr equation, is much greater than any series or numerical solution can provide.

7.2. *Perturbation's linearized dynamics at near-critical swirl ratios*

We can also consider the long-wave asymptotic approach for the solution of the linearized governing equations (2.5). We assume that the streamfunction of the perturbation $\psi_1(x, y, t)$ is of the form

$$\psi_1(x, y, t) = \phi_B(y)\mathscr{A}(X, t^*) + O(\epsilon), \tag{7.1}$$

with $\epsilon = 1/L^2$, rescaled length $X = x/L$ and rescaled time $t^* = t/\epsilon^{3/2}$, as introduced in § 3.1. Through a similar asymptotic analysis at near-critical swirl ratios, it can be

shown that the dynamics of the perturbation function $\mathscr{A}(X, t^*)$ is described by

$$\mathscr{A}_{t^*} = \frac{1}{\tau}\mathscr{A}_{XXX} + \frac{\kappa_\omega \beta}{\tau}\mathscr{A}_X, \tag{7.2}$$

where τ, κ_ω and β are defined in § 3.1. We consider the perturbation dynamics under various inlet–outlet boundary conditions.

For the case where the periodic inlet–outlet conditions are imposed at the pipe inlet and outlet, the problem (7.2) depicts a conservative perturbation dynamics. This is found from multiplying (7.2) by $\mathscr{A}$ and integrating the result over the axial interval [0, 1]; one obtains

$$\begin{aligned}\frac{1}{2}\frac{\mathrm{d}}{\mathrm{d}t^*}\int_0^1 \mathscr{A}^2\,\mathrm{d}X &= -\int_0^1 \frac{1}{\tau}\mathscr{A}_X\mathscr{A}_{XX}\,\mathrm{d}X + \frac{1}{\tau}\mathscr{A}\mathscr{A}_{XX}\Big|_{X=0}^{X=1} + \frac{\kappa_\omega\beta}{\tau}\frac{\mathscr{A}^2}{2}\Big|_{X=0}^{X=1} \\ &= -\frac{1}{\tau}\frac{\mathscr{A}_X^2}{2}\Big|_{X=0}^{X=1} + \frac{1}{\tau}\mathscr{A}\mathscr{A}_{XX}\Big|_{X=0}^{X=1} + \frac{\kappa_\omega\beta}{\tau}\frac{\mathscr{A}^2}{2}\Big|_{X=0}^{X=1}.\end{aligned} \tag{7.3}$$

It is clear that

$$\frac{\mathrm{d}}{\mathrm{d}t^*}\int_0^1 \mathscr{A}^2\,\mathrm{d}X = 0, \tag{7.4}$$

when the periodic inlet–outlet conditions are imposed. Thus, $\int_0^1 \mathscr{A}^2\,\mathrm{d}X$, which is proportional to the kinetic energy of the disturbance, is conserved for all time. The result (7.4) implies the linear stability of the base flow at near-critical swirl ratios under the periodic conditions. Note that the conservation nature of the full linearized equations (2.5) is retained by (7.2).

We now consider the perturbation dynamics under non-periodic conditions imposed at the pipe inlet and outlet. One notices that (7.2) contains the third-order dispersive term $\mathscr{A}_{XXX}$. Therefore, three boundary conditions must be imposed at the pipe inlet and outlet, among them two are imposed at the inlet and one at the outlet, to form a well-posed problem. The necessary non-symmetric treatment of the boundary conditions at the inlet and outlet is likely to break up the conservative nature of the perturbation dynamics and leads to the change of the vortex stability around the critical swirl. We consider the two possible cases of conditions studied above.

For the boundary conditions $\mathscr{A}(0, t^*) = \mathscr{A}(1, t^*) = 0$ and $\mathscr{A}_{XX}(0, t^*) = 0$, we find from (7.3) that

$$\frac{1}{2}\frac{\mathrm{d}}{\mathrm{d}t^*}\int_0^1 \mathscr{A}^2\,\mathrm{d}X = \frac{1}{\tau}\frac{\mathscr{A}_X^2(0, t^*) - \mathscr{A}_X^2(1, t^*)}{2}. \tag{7.5}$$

The terms on the right-hand side of (7.5) depend at all time on the boundary values $\mathscr{A}_X(0, t^*)$ and $\mathscr{A}_X(1, t^*)$. These are not specified by the boundary conditions and are, therefore, subject to the evolution of the perturbation function $\mathscr{A}$. The linear stability analysis in § 3.2 shows that indeed the dominant mode of perturbation for this set of boundary conditions is stable and $\mathscr{A}_X^2(0, t^*) < \mathscr{A}_X^2(1, t^*)$ for $\omega < \omega_1$ and is unstable and $\mathscr{A}_X^2(0, t^*) > \mathscr{A}_X^2(1, t^*)$ for $\omega > \omega_1$. The physical implication of this result is that the flow instability may be controlled by restraining the magnitude of the radial velocity at the inlet. In fact, in this case, a flow control approach, which imposes a radial velocity at the inlet related with $\mathscr{A}_X(0, t^*)$ such that for all time $|\mathscr{A}_X(0, t^*)| \leqslant |\mathscr{A}_X(1, t^*)|$, instead of $\mathscr{A}_{XX}(0, t) = 0$, would stabilize the flow.

For the boundary conditions $\mathscr{A}(0,t^*)=\mathscr{A}_X(1,t^*)=0$ and $\mathscr{A}_{XX}(0,t^*)=0$, we have

$$\frac{1}{2}\frac{\mathrm{d}}{\mathrm{d}t^*}\int_0^1 \mathscr{A}^2\,\mathrm{d}X=\frac{1}{\tau}\frac{\mathscr{A}_X^2(0,t^*)}{2}+\frac{1}{\tau}\mathscr{A}(1,t^*)\mathscr{A}_{XX}(1,t^*)+\frac{\kappa_\omega\beta}{\tau}\frac{\mathscr{A}^2(1,t^*)}{2}. \tag{7.6}$$

The terms on the right-hand side of (7.6) depend at all time on the boundary values $\mathscr{A}_X(0,t^*)$, $\mathscr{A}(1,t^*)$ and $\mathscr{A}_{XX}(1,t^*)$. Again, these are not specified by the boundary conditions and are, therefore, subject to the evolution of the perturbation function $\mathscr{A}$. In this case, the dominant term is the term related to κ_ω. The linear stability analysis in § 3.2 shows that when $\kappa_\omega<\kappa_{\omega,1}$ (or $\omega<\omega_1$), this term is negative and causes the decay of the perturbation. When $\kappa_\omega>\kappa_{\omega,1}$ (or $\omega>\omega_1$), this term is sufficiently positive and destabilizes the flow.

Remark 7.1. The result (7.3) sheds further light on the dynamics of the flow. Consider, for example, the case where the boundary conditions are given by

$$\mathscr{A}(0,t^*)=\mathscr{A}_X(0,t^*)=0 \quad \text{and} \quad \mathscr{A}(1,t^*)=0. \tag{7.7}$$

Note that we simply replace the inlet condition $\mathscr{A}_{XX}(0,t^*)=0$ with $\mathscr{A}_X(0,t^*)=0$, which specifies a vanishing radial velocity at the inlet for all time. One finds, for this case,

$$\frac{\mathrm{d}}{\mathrm{d}t^*}\int_0^1 \mathscr{A}^2\,\mathrm{d}X=-\frac{1}{\tau}\frac{\mathscr{A}_X(1,t^*)^2}{2}, \tag{7.8}$$

which is negative for all time. Thus, the flow under these boundary conditions is always asymptotically stable. A similar result was found in Gallaire & Chomaz (2004) for the solid-body rotation flow.

Remark 7.2. Another case of interest is where the boundary conditions are given by

$$\mathscr{A}(0,t^*)=\mathscr{A}_X(0,t^*)=0 \quad \text{and} \quad \mathscr{A}_X(1,t^*)=0. \tag{7.9}$$

Here, again we replace the inlet condition $\mathscr{A}_{XX}(0,t^*)=0$ with $\mathscr{A}_X(0,t^*)=0$, which specifies a vanishing radial velocity at the inlet and the outlet for all time. This set of boundary conditions has recently been studied by Leclaire & Sipp (2010). One finds, for this case,

$$\frac{\mathrm{d}}{\mathrm{d}t^*}\int_0^1 \mathscr{A}^2\,\mathrm{d}X=\frac{1}{\tau}\mathscr{A}(1,t^*)\mathscr{A}_{XX}(1,t^*)+\frac{\kappa_\omega\beta}{\tau}\frac{\mathscr{A}^2(1,t^*)}{2}. \tag{7.10}$$

The terms on the right-hand side of (7.10) depend at all time on the boundary values $\mathscr{A}(1,t^*)$ and $\mathscr{A}_{XX}(1,t^*)$. Again, these are not specified by the boundary conditions and are, therefore, subject to the evolution of the perturbation function $\mathscr{A}$. In this case, again, the dominant term is the term related to κ_ω. Leclaire & Sipp (2010) found that the critical κ_ω in this case is higher than the critical values for the cases mentioned above. As found in their analysis, indeed, when κ_ω is less than this critical number, this term is negative and causes the decay of the perturbation. When κ_ω is greater than this critical number, this term is sufficiently positive and destabilizes the flow.

The fact that $(\mathrm{d}/\mathrm{d}t^*)\int_0^1 \mathscr{A}^2\,\mathrm{d}X$ is solely determined by the boundary terms of the time-dependent solution of the linear governing equation, does not imply that the energy transfer between the disturbance and the base flow occurs only at the boundary. On the contrary, a kinetic energy transfer does take place at the pipe inlet and outlet as well as inside the domain, as shown in § 6. This situation can be explained by the fact that there exists a strong coupling of the kinetic energy transfer

mechanism between the boundary and the internal flow. The terms that appear on the right-hand side of (7.5) and (7.6) comprise the combined contribution from both the boundary and the internal flow to the perturbation's kinetic energy production. Note that the basic stability equation (3.8) is but a solvability condition for the ϵ^2 order stability equation (3.7). See also Remark 6.1.

The principal mechanism for the perturbation's energy production is analysed in § 6 using the Reynold–Orr equation. This enables one to pinpoint where and how the perturbation's kinetic energy is produced. We have found the following points.

(*a*) At the pipe inlet and outlet, the perturbation's kinetic energy production is generated through the flow convection and the work performed on the perturbation by the pressure perturbation. See (6.4) and (6.5) for the detailed expressions of the kinetic energy production terms at the boundaries.

(*b*) Inside the flow domain the perturbation's kinetic energy production is generated through the interaction of the velocity field of the perturbation and the strain-rate field of the base flow, regulated by the Reynold–Orr equation. See (6.4) and (6.5) for the detailed expressions of the kinetic energy production terms in the bulk. The underlying physics is that the presence of the non-periodic boundary conditions at the inlet and outlet applies a change of flow force on the flow, alters naturally the perturbation's mode shape, and thereby induces the internal energy transfer in the domain. This type of internal kinetic energy transfer is a generic behaviour of vortex flows and exists in general swirling flows confined in a finite-length pipe, except for the special case of the strain-free solid-body rotation with a uniform axial flow.

This discussion consolidates our view that the Rayleigh stability mechanism of a swirling flow would be eliminated for the flow that is confined in a finite-length pipe. With the influence of the physical non-periodic boundary conditions at the pipe inlet and outlet, the perturbation is robustly engaged in kinetic energy transfer with the base flow at the inlet and outlet as well as inside the domain. The neutrally stable vortex flow according to Rayleigh's stability analysis is either asymptotically stable or unstable, depending on the net perturbation's kinetic energy production as a function of the swirl ratio. This perturbation's kinetic energy production mechanism governs the WR instability.

8. Conclusions

The rate of change of the perturbation's kinetic energy E of a perturbed columnar and near-critical swirling flow in a finite-length pipe with periodic and non-periodic inlet–outlet conditions can be analysed by an asymptotic approach for a long pipe. A novel asymptotic solution of the linear stability of a flow in a long pipe has been developed and provides the dominant perturbation's mode shape and growth rate. This solution technique is general and can be applied to any vortex flow profile, in a range of swirl levels around the critical level for vortex breakdown, and for various outlet conditions. The solutions of the perturbation's mode shape can be used in a modified form of the Reynolds–Orr equation to estimate the production (or loss) of the perturbation's kinetic energy E at the pipe boundaries and inside the domain. The analysis provides a new energy-based understanding of the WR vortex instability mechanism and the exchange of global stability around the critical swirl ω_1. The complex interaction between the various production terms of E is demonstrated. It is found that the solid-body rotation is a special case where the production of the perturbation's kinetic energy vanishes and the stability is determined only by the asymmetric transfer of E at the boundaries. For a general vortex flow, the production

of E inside the domain competes with the transfer of E at the boundaries to determine the flow stability.

The present analysis shows that the production of E inside the domain plays an important role in the WR instability mechanism. For a general base flow, the perturbation's mode shape develops natural deviations with respect to the pipe inlet (or outlet) in response to the non-periodic inlet–outlet conditions. These deviations affect the production of E inside the domain and at the boundaries and form a critical balance of production of E from the base flow that governs the flow stability around the critical state. The flow in the domain is active in convecting the perturbations from the inlet to the outlet as well as affecting their size and growth rate by engaging with the base flow strain rates to produce (or lose) their kinetic energy. Real flow effects such as pipe divergence or contraction, slight viscosity, inlet vorticity disturbances, weak reaction and compressibility may result in similar effects that also alter the production of energy inside the domain and promote (or delay) the onset of instability at swirl ratios below (or above) the critical level. It is proposed to use the energy considerations presented in this paper for the future design of active control systems of the stability of vortex flows in pipes that either promote or delay the Wang–Rusak instability.

Appendix A. The inlet condition

Using the radial momentum equation for a steady, inviscid and incompressible axisymmetric swirling flow in axisymmetric coordinates, $uu_r + wu_x - v^2/r = -p_r$, with the given inlet conditions $u_x(0, r) = 0$, $v(0, r) = \omega v_0(r)$, $w(0, r) = w_0(r)$, $p(0, 0) = p_0$, we find that the profile of the inlet pressure is given by

$$p(0, r) = p_0 + \omega^2 \int_0^r \frac{v_0^2(r')}{r'}\,\mathrm{d}r' - \frac{1}{2}u^2(0, r), \tag{A 1}$$

for $0 \leqslant r \leqslant 1$. The total head $H = p + (1/2)(u^2 + v^2 + w^2)$ profile at the inlet is

$$\begin{aligned} H(0, r) &= p(0, r) + \frac{1}{2}\left(u^2(0, r) + v^2(0, r) + w^2(0, r)\right) \\ &= p_0 + \omega^2 \int_0^r \frac{v_0^2(r')}{r'}\,\mathrm{d}r' + \frac{1}{2}\left(\omega^2 v_0^2(r) + w_0^2(r)\right), \end{aligned} \tag{A 2}$$

for $0 \leqslant r \leqslant 1$. It shows that for all ω, under the given inlet conditions, $H(0, r)$ does not change with the solution of the flow inside the domain even though the solution may exhibit a non-zero radial velocity $u(0, r)$ at the inlet. Therefore, this set of pipe inlet conditions describes for all ω a total head-conserving apparatus which can be physically realized.

On the other hand, if the inlet condition $u_x(0, r) = 0$ is replaced by a zero radial velocity at the inlet $u(0, r) = 0$ used by Leclaire & Sipp (2010), we have

$$p(0, r) = p_0 + \omega^2 \int_0^r \frac{v_0^2(r')}{r'}\,\mathrm{d}r' - \int_0^r w_0 u_x(0, r')\,\mathrm{d}r', \tag{A 3}$$

for $0 \leqslant r \leqslant 1$. The total head $H = p + (1/2)(u^2 + v^2 + w^2)$ profile at the inlet in this case is

$$\begin{aligned} H(0, r) &= p(0, r) + \frac{1}{2}(v^2(0, r) + w^2(0, r)) \\ &= p_0 + \omega^2 \int_0^r \frac{v_0^2(r')}{r'}\,\mathrm{d}r' + \frac{1}{2}\left(\omega^2 v_0^2(r) + w_0^2(r)\right) - \int_0^r w_0 u_x(0, r')\,\mathrm{d}r', \end{aligned} \tag{A 4}$$

for $0 \leqslant r \leqslant 1$. It shows that for all ω, under the given inlet conditions, $H(0, r)$ changes with the solution of the flow inside the domain since the solution will exhibit a non-zero axial gradient of the radial velocity $u_x(0, r)$ at the inlet. This set of pipe inlet conditions describes a situation where the total head is non-conserving. This is not a natural situation and as such requires an apparatus with special (non-trivial) adjustments upstream of the pipe to be physically realized.

Appendix B. The Reynolds–Orr equation for a swirling flow in a straight long pipe

We develop an asymptotic form of the Reynolds–Orr equation from the asymptotic solution of the stability equation. We first derive the perturbation's velocity field.

B.1. *The perturbation's velocity field*

From the streamfunction relationship with the radial and axial velocity components and the perturbation's form (2.4), we have $u_1 = -\epsilon_1 \psi_{1x}/\sqrt{2y} + \cdots$ and $w_1 = \epsilon_1 \psi_{1y} + \cdots$. From the perturbation's mode shape (2.7), $u_1 = -\epsilon_1(\phi_{1x}/\sqrt{2y})\,\mathrm{e}^{\sigma t} + \cdots$ and $w_1 = \epsilon_1 \phi_{1y} \mathrm{e}^{\sigma t} + \cdots$. Therefore, using (6.5), $\bar{u}_1 = -\sqrt{\epsilon}(\phi_X/\sqrt{2y})$ and $\bar{w}_1 = \phi_y$. From the perturbation's asymptotic shape for a long pipe (3.1), we have

$$\left.\begin{aligned} \bar{u}_1(X, y; \sigma^*) &= -\frac{1}{\sqrt{2y}}(\epsilon^{1/2}\phi_B(y)A_X + \epsilon^{3/2}\bar{\phi}_X) + O(\epsilon^{5/2}), \\ \bar{w}_1(X, y; \sigma^*) &= \phi_{By}A + \epsilon\bar{\phi}_y + O(\epsilon^2). \end{aligned}\right\} \tag{B 1}$$

Also, from the relationship between the circulation function and the circumferential velocity, we have $v = K/\sqrt{2y}$ and, from (2.4) and (2.7), $v_1 = \epsilon_1 K_1/\sqrt{2y} = \epsilon_1 k/\sqrt{2y}\,\mathrm{e}^{\sigma t}$. Then, using (6.5), $\bar{v}_1 = k/\sqrt{2y}$. The linearized circulation equation in (2.5) gives

$$K_1(x, y, t) = \frac{2y^2}{\omega K_0(y)} \int_0^x (\chi_{1t} + \psi_{0y}\chi_{1x} - \chi_{0y}\psi_{1x})\,\mathrm{d}x, \tag{B 2}$$

where $\chi_1 = -(\psi_{1yy} + \psi_{1xx}/2y)$. Let $\chi_1 = \epsilon_1 \chi^+ \mathrm{e}^{\sigma t}$, where $\chi^+ = -(\phi_{yy} + \phi_{xx}/2y)$. Inserting this, (2.7), and $\sigma = \epsilon^{3/2}\sigma^*$ into (B 2) and using the inlet conditions (2.9) yields

$$k(X, y; \sigma^*) = \frac{2y^2}{\omega K_0(y)} \left(\epsilon\sigma^* \int_0^X \chi^+ \,\mathrm{d}X' + \psi_{0y}\chi^+ - \chi_{0y}\phi\right). \tag{B 3}$$

Using (3.1), $\chi^+ = -\phi_{Byy}A - \epsilon(\phi_B A_{XX}/2y + \bar{\phi}_{XX}) + O(\epsilon^2)$. Substituting this and (3.1) in (B 3) gives

$$\begin{aligned} k(X, y; \sigma^*) = \frac{2y^2}{\sqrt{\Omega_B} K_0(y)} \Bigg[& -\left(\psi_{0y}\phi_{Byy} + \chi_{0y}\phi_B\right)A \\ & - \epsilon\left(\sigma^*\phi_{Byy}\int_0^X A(X'; \sigma^*)\,\mathrm{d}X' + (\psi_{0y}\bar{\phi}_{yy} + \chi_{0y}\bar{\phi}) + \psi_{0y}\frac{\phi_B}{2y}A_{XX}\right)\Bigg] \\ & + \epsilon\frac{\kappa_\omega y^2}{\Omega_B^{3/2}}(\psi_{0y}\phi_{Byy} + \chi_{0y}\phi_B)A + O(\epsilon^2). \end{aligned} \tag{B 4}$$

From (B 4) we obtain

$$\bar{v}_1(X, y; \sigma^*) = \frac{\sqrt{2}y^{3/2}}{\sqrt{\Omega_B}K_0(y)}\Bigg[-(\psi_{0y}\phi_{Byy} + \chi_{0y}\phi_B)A + \epsilon\Bigg(-\sigma^*\phi_{Byy}\int_0^X A(X';\sigma^*)\,\mathrm{d}X' - (\psi_{0y}\bar{\phi}_{yy} + \chi_{0y}\bar{\phi}) - \psi_{0y}\frac{\phi_B}{2y}A_{XX} + \frac{\kappa_\omega}{2\Omega_B}(\psi_{0y}\phi_{Byy} + \chi_{0y}\phi_B)A\Bigg)\Bigg] + O(\epsilon^2). \tag{B 5}$$

Integrating (3.7) twice with respect to X, and using the inlet conditions (3.3), (3.5) and $A(0;\sigma^*) = A_{XX}(0;\sigma^*) = 0$, results in

$$\bar{\phi}_{yy} + \left(\Omega_B\frac{K_0K_{0y}}{2y^2\psi_{0y}^2} + \frac{\chi_{0y}}{\psi_{0y}}\right)\bar{\phi} + \frac{\phi_B}{2y}A_{XX} + \kappa_\omega\frac{K_0K_{0y}}{2y^2\psi_{0y}^2}\phi_B A - \sigma^*\left(\Omega_B\frac{K_0K_{0y}}{y^2\psi_{0y}^3} + \frac{\chi_{0y}}{\psi_{0y}^2}\right)\phi_B\int_0^X A(X;\sigma^*)\,\mathrm{d}X' = 0. \tag{B 6}$$

Using (B 6) and

$$\phi_{Byy} + \frac{\chi_{0y}}{\psi_{0y}}\phi_B = -\Omega_B\frac{K_0K_{0y}}{2y^2\psi_{0y}^2}\phi_B, \tag{B 7}$$

the expression (B 5) can be written in a compact form

$$\bar{v}_1(X, y; \sigma^*) = \frac{\sqrt{\Omega_B}K_{0y}}{\sqrt{2y}\psi_{0y}}\phi_B A + \epsilon\left[\frac{\sqrt{\Omega_B}K_{0y}}{\sqrt{2y}\psi_{0y}}\phi_B\left(\frac{\kappa_\omega}{2\Omega_B}A - \frac{\sigma^*}{\psi_{0y}}\int_0^X A(X';\sigma^*)\,\mathrm{d}X'\right) + \frac{\sqrt{\Omega_B}K_{0y}}{\sqrt{2y}\psi_{0y}}\bar{\phi}\right] + O(\epsilon^2). \tag{B 8}$$

B.2. *Asymptotic form of the terms in the Reynolds–Orr equation*

In the following, the asymptotic expressions for the various terms in the Reynolds–Orr equation (5.7) are derived.

1. E_{uv}: Inserting u_1 and v_1 from (6.1), (6.2) and $\omega = \sqrt{\Omega_B + \kappa_\omega\epsilon}$ in (5.8), and arranging the terms in the corresponding orders, gives

$$\begin{aligned}
E_{uv} &= \epsilon_1^2\,\mathrm{e}^{\sigma^* t^*}\left[-\sqrt{\Omega_B + \kappa_\omega\epsilon}\int_0^1\int_0^{1/2}\left(\frac{K_{0y} - K_0}{y}\right)\bar{u}_1\bar{v}_1\,\mathrm{d}y\,\mathrm{d}X\right] + \cdots \\
&= \epsilon_1^2\,\mathrm{e}^{\sigma^* t^*}\Bigg[-\Omega_B\int_0^1\int_0^{1/2}\left(\frac{K_0}{y} - K_{0y}\right)\frac{K_{0y}}{2y\psi_{0y}}\phi_B^2 A A_X\,\mathrm{d}y\,\mathrm{d}X \\
&\quad -\epsilon\Bigg[\Omega_B\int_0^1\int_0^{1/2}\left(\frac{K_0}{y} - K_{0y}\right)\frac{K_{0y}}{2y\psi_{0y}}\phi_B^2 \\
&\quad \times\left(\frac{\kappa_\omega}{2\Omega_B}A - \frac{\sigma^*}{\psi_{0y}}\int_0^X A(X';\sigma^*)\,\mathrm{d}X'\right)A_X\,\mathrm{d}y\,\mathrm{d}X \\
&\quad +\Omega_B\int_0^1\int_0^{1/2}\left(\frac{K_0}{y} - K_{0y}\right)\frac{K_{0y}}{2y\psi_{0y}}\phi_B(A_X\bar{\phi} + A\bar{\phi}_X)\,\mathrm{d}y\,\mathrm{d}X \\
&\quad +\kappa_\omega\int_0^1\int_0^{1/2}\left(\frac{K_0}{y} - K_{0y}\right)\frac{K_{0y}}{4y\psi_{0y}}\phi_B^2 A A_X\,\mathrm{d}y\,\mathrm{d}X\Bigg] + O(\epsilon^2)\Bigg] + \cdots .
\end{aligned} \tag{B 9}$$

Using $A(0;\sigma^*)=0$,

$$\left.\begin{aligned}\int_0^1 AA_X\,\mathrm{d}X &= \frac{1}{2}A^2(1;\sigma^*),\\ \int_0^1 A_X\int_0^X A(X';\sigma^*)\,\mathrm{d}X' &= A(1;\sigma^*)\int_0^1 A\,\mathrm{d}X-\int_0^1 A^2\,\mathrm{d}X,\end{aligned}\right\} \tag{B 10}$$

leads to

$$\begin{aligned}E_{uv}=\epsilon_1^2\,\mathrm{e}^{\sigma^* t^*}\Bigg[&-\frac{1}{2}\Omega_B\left(\int_0^{1/2}\left(\frac{K_0}{y}-K_{0y}\right)\frac{K_{0y}}{2y\psi_{0y}}\phi_B^2\,\mathrm{d}y\right)A^2(1;\sigma^*)\\ &-\epsilon\Bigg[\frac{1}{2}\kappa_\omega\left(\int_0^{1/2}\left(\frac{K_0}{y}-K_{0y}\right)\frac{K_{0y}}{2y\psi_{0y}}\phi_B^2\,\mathrm{d}y\right)A^2(1;\sigma^*)\\ &-\sigma^*\Omega_B\left(\int_0^{1/2}\left(\frac{K_0}{y}-K_{0y}\right)\frac{K_{0y}}{2y\psi_{0y}^2}\phi_B^2\,\mathrm{d}y\right)\left(A(1;\sigma^*)\int_0^1 A\,\mathrm{d}X-\int_0^1 A^2\,\mathrm{d}X\right)\\ &+\Omega_B\left(\int_0^{1/2}\left(\frac{K_0}{y}-K_{0y}\right)\frac{K_{0y}}{2y\psi_{0y}}\phi_B\bar{\phi}(1,y;\sigma^*)\,\mathrm{d}y\right)A(1;\sigma^*)\Bigg]+O(\epsilon^2)\Bigg]+\cdots.\end{aligned} \tag{B 11}$$

2. E_{uw}: Inserting u_1 and w_1 from (6.1), (6.2) and $-w_{0y}=\chi_0$ in (5.8) gives

$$\begin{aligned}E_{uw}&=\epsilon_1^2\,\mathrm{e}^{2\sigma^* t^*}\left[\int_0^1\int_0^{1/2}\sqrt{2y}\chi_0\bar{u}_1\bar{w}_1\,\mathrm{d}y\,\mathrm{d}X\right]+\cdots\\ &=-\epsilon_1^2\,\mathrm{e}^{2\sigma^* t^*}\left[\int_0^1\int_0^{1/2}\chi_0(\phi_B A_X+\epsilon\bar{\phi}_X+O(\epsilon^2))(\phi_{By}A+\epsilon\bar{\phi}_y+O(\epsilon^2))\,\mathrm{d}y\,\mathrm{d}X\right]+\ldots\\ &=\epsilon_1^2\,\mathrm{e}^{2\sigma^* t^*}\Bigg[\frac{1}{2}\left(\int_0^{1/2}\chi_{0y}\phi_B^2\,\mathrm{d}y\right)A^2(1;\sigma^*)\\ &\quad-\epsilon\int_0^1\int_0^{1/2}\chi_0(\bar{\phi}_X\phi_{By}A+\bar{\phi}_y\phi_B A_X)\,\mathrm{d}y\,\mathrm{d}X+O(\epsilon^2)\Bigg]+\cdots.\end{aligned} \tag{B 12}$$

Here we used $\int_0^{1/2}\chi_0\phi_B\phi_{By}\,\mathrm{d}y=-\frac{1}{2}\int_0^{1/2}\chi_{0y}\phi_B^2\,\mathrm{d}y$. To further explore the term $O(\epsilon)$ in (B 12), we integrate (3.7) twice with respect to X and use the inlet conditions (3.5), then (3.3), and then $A(0;\sigma^*)=A_{XX}(0;\sigma^*)$, and find

$$\begin{aligned}\bar{\phi}_{yy}+\left(\Omega_B\frac{K_0K_{0y}}{2y^2\psi_{0y}^2}-\frac{\psi_{0yyy}}{\psi_{0y}}\right)\bar{\phi}+\frac{\phi_B}{2y}A_{XX}+\kappa_\omega\frac{K_0K_{0y}}{2y^2\psi_{0y}^2}\phi_B A\\ -\sigma^*\left(\Omega_B\frac{K_0K_{0y}}{y^2\psi_{0y}^3}+\frac{\chi_{0y}}{\psi_{0y}^2}\right)\phi_B\int_0^X A(X';\sigma^*)\,\mathrm{d}X'=0.\end{aligned} \tag{B 13}$$

Multiplying (B 13) by $\psi_{0y}\phi_B A_X$, using (3.2), and then integrating the result over the domain $0 \leqslant X \leqslant 1$ and $0 \leqslant y \leqslant 1/2$ gives

$$\int_0^1\int_0^{1/2}(\bar{\phi}_{yy}\phi_B - \bar{\phi}\phi_{Byy})\psi_{0y}A_X\,\mathrm{d}y\,\mathrm{d}X + \int_0^1\int_0^{1/2}\psi_{0y}\frac{\phi_B^2}{2y}A_{XX}A_X\,\mathrm{d}y\,\mathrm{d}X + \kappa_\omega\int_0^1\int_0^{1/2}\frac{K_0K_{0y}}{2y^2\psi_{0y}}\phi_B^2AA_X\,\mathrm{d}y\,\mathrm{d}X - \sigma^*\int_0^1\int_0^{1/2}\left(2\Omega_B\frac{K_0K_{0y}}{2y^2\psi_{0y}^2}+\frac{\chi_{0y}}{\psi_{0y}}\right)\phi_B^2\left(\int_0^X A(X';\sigma^*)\,\mathrm{d}X'\right)A_X\,\mathrm{d}y\,\mathrm{d}X = 0. \quad \text{(B 14)}$$

Through twice integrating the first term in (B 14) by parts, one time with respect to X and then with respect to y, and the use of inlet conditions (3.3) and $A(0;\sigma^*)=0$ we find that

$$\int_0^1\int_0^{1/2}\left(\bar{\phi}_{yy}\phi_B - \bar{\phi}\phi_{Byy}\right)\psi_{0y}A_X\,\mathrm{d}y\,\mathrm{d}X = \int_0^1\int_0^{1/2}\chi_0(\bar{\phi}_X\phi_{By}A + \bar{\phi}_y\phi_BA_X)\,\mathrm{d}y\,\mathrm{d}X - \left(\int_0^{1/2}\chi_0\phi_{By}\bar{\phi}(1,y;\sigma^*)\,\mathrm{d}y\right)A(1;\sigma^*). \quad \text{(B 15)}$$

Using (B 15) and the integrals $\int_0^1 A_{XX}A_X\,\mathrm{d}X = \frac{1}{2}(A_X^2(1;\sigma^*) - A_X^2(0;\sigma^*))$, $\int_0^1 AA_X\,\mathrm{d}X = \frac{1}{2}A^2(1;\sigma^*)$, and $\int_0^1 A_X\int_0^X A(X';\sigma^*\,\mathrm{d}X')\,\mathrm{d}X = A(1;\sigma^*)\int_0^1 A\,\mathrm{d}X - \int_0^1 A^2\,\mathrm{d}X$ in (B 14) and this in (B 12), we find

$$E_{uw} = \epsilon_1^2\,\mathrm{e}^{2\sigma^*t^*}\left[\frac{1}{2}\left(\int_0^{1/2}\chi_{0y}\phi_B^2\,\mathrm{d}y\right)A^2(1;\sigma^*) - \epsilon\left[\frac{1}{2}\kappa_\omega\left(\int_0^{1/2}\frac{K_0K_{0y}}{2y^2\psi_{0y}}\phi_B^2\,\mathrm{d}y\right)A^2(1;\sigma^*) + \frac{1}{2}\left(\int_0^{1/2}\psi_{0y}\frac{\phi_B^2}{2y}\,\mathrm{d}y\right)\left(A_X^2(1;\sigma^*) - A_X^2(0;\sigma^*)\right) - \sigma^*\left(\int_0^{1/2}\left(2\Omega_B\frac{K_0K_{0y}}{2y^2\psi_{0y}^2}+\frac{\chi_{0y}}{\psi_{0y}}\right)\phi_B^2\,\mathrm{d}y\right)\left(A(1;\sigma^*)\int_0^1 A\,\mathrm{d}X - \int_0^1 A^2\,\mathrm{d}X\right) - \left(\int_0^{1/2}\chi_0\phi_{By}\bar{\phi}(1,y;\sigma^*)\,\mathrm{d}y\right)A(1;\sigma^*)\right] + O(\epsilon^2)\right] + \cdots. \quad \text{(B 16)}$$

3. $E_{uu_{inlet}}$: Inserting $u_1(0,y,t) = -\epsilon_1\,\mathrm{e}^{\sigma^*t^*}(1/\sqrt{2y})(\epsilon^{1/2}\phi_B(y)A_X(0;\sigma^*)+\cdots)$ in (5.8) gives

$$E_{uu_{inlet}} = -\frac{1}{2}\epsilon_1^2\,\mathrm{e}^{2\sigma^*t^*}\left[\epsilon\left(\int_0^{1/2}\psi_{0y}\frac{\phi_B^2}{2y}\,\mathrm{d}y\right)A_X^2(0;\sigma^*) + O(\epsilon^2)\right] + \cdots. \quad \text{(B 17)}$$

4. $E_{uu_{outlet}}$: Inserting $u_1(L,y,t) = -\epsilon_1\,\mathrm{e}^{\sigma^*t^*}(1/\sqrt{2y})(\epsilon^{1/2}\phi_B(y)A_X(1;\sigma^*)+\cdots)$ in (5.8) gives

$$E_{uu_{outlet}} = -\frac{1}{2}\epsilon_1^2\,\mathrm{e}^{2\sigma^*t^*}\left[\epsilon\left(\int_0^{1/2}\psi_{0y}\frac{\phi_B^2}{2y}\,\mathrm{d}y\right)A_X^2(1;\sigma^*) + O(\epsilon^2)\right] + \cdots. \quad \text{(B 18)}$$

5. $E_{vv_{outlet}}$: Inserting $v_1(L, y, t) = \epsilon_1 \mathrm{e}^{\sigma^* t^*} \bar{v}_1(1, y; \sigma^*) + \cdots$ in (5.8) and using (B 8) gives

$$\begin{aligned} E_{vv_{outlet}} &= -\frac{1}{2}\epsilon_1^2 \mathrm{e}^{2\sigma^* t^*} \int_0^{1/2} w_0 \bar{v}_1^2(1, y; \sigma^*)\, \mathrm{d}y \\ &= -\frac{1}{2}\epsilon_1^2 \mathrm{e}^{2\sigma^* t^*} \left[\Omega_B \left(\int_0^{1/2} \frac{K_{0y}^2}{2y\psi_{0y}} \phi_B^2 \, \mathrm{d}y \right) A^2(1; \sigma^*) \right. \\ &\quad - \epsilon \left[\frac{1}{2}\kappa_\omega \left(\int_0^{1/2} \frac{K_{0y}^2 \phi_B^2}{2y\psi_{0y}} \, \mathrm{d}y \right) A^2(1; \sigma^*) \right. \\ &\quad - \sigma^* \Omega_B \left(\int_0^{1/2} \frac{K_{0y}^2 \phi_B^2}{2y\psi_{0y}} \, \mathrm{d}y \right) \left(A(1; \sigma^*) \int_0^1 A \, \mathrm{d}X \right) \\ &\quad \left. \left. + \Omega_B \left(\int_0^{1/2} \frac{K_{0y}^2}{2y\psi_{0y}} \phi_B \bar{\phi}(1, y; \sigma^*) \, \mathrm{d}y \right) A(1; \sigma^*) \right] + O(\epsilon^2) + \cdots \right]. \end{aligned} \tag{B 19}$$

6. $E_{ww_{outlet}}$: Inserting $w_1(L, y, t) = \epsilon_1 \mathrm{e}^{\sigma^* t^*} \bar{w}_1(1, y; \sigma^*) + \cdots$ in (5.8) and using (B 1) gives

$$\begin{aligned} E_{w_{outlet}} &= -\frac{1}{2}\epsilon_1^2 \mathrm{e}^{2\sigma^* t^*} \left[\int_0^{1/2} w_0 \bar{w}_1^2(1, y; \sigma *) \, \mathrm{d}y \right] + \cdots \\ &= -\frac{1}{2}\epsilon_1^2 \mathrm{e}^{2\sigma^* t^*} \left[\int_0^{1/2} \psi_{0y} \phi_{By}^2 \, \mathrm{d}y \right. \\ &\quad \left. + 2\epsilon \left(\int_0^{1/2} \psi_{0y} \phi_{By} \bar{\phi}_y(1, y; \sigma^*) \, \mathrm{d}y \right) A(1; \sigma^*) + O(\epsilon^*) \right] + \cdots . \end{aligned} \tag{B 20}$$

Using

$$\phi_{Byy} = -\left(\frac{\omega_B^2 K_0 K_{0y}}{2y^2 \psi_{0y}^2} + \frac{\chi_{0y}}{\psi_{0y}} \right) \phi_B, \tag{B 21}$$

$w_{0y} = -\chi_0$ and $w_{0yy} = -\chi_{0y}$, then twice integrating by parts and applying the boundary conditions $\phi_B(0) = \phi_B(1/2) = 0$, gives

$$\begin{aligned} -\int_0^{1/2} \psi_{0y} \phi_{By}^2 \, \mathrm{d}y &= \int_0^{1/2} (\psi_{0yy} \phi_{By} + \psi_0 \phi_{Byy}) \phi_B \, \mathrm{d}y = \int_0^{1/2} \left(\psi_{0y} \phi_{Byy} \phi_B + \frac{1}{2}\chi_{0y} \phi_B^2 \right) \mathrm{d}y \\ &= -\int_0^{1/2} \left(\Omega_B \frac{K_0 K_{0y}}{2y^2 \psi_{0y}} + \frac{1}{2}\chi_{0y} \right) \phi_B^2 \, \mathrm{d}y \end{aligned} \tag{B 22}$$

and

$$\begin{aligned} -\int_0^{1/2} \psi_{0y} \phi_{By}(y) \bar{\phi}_y(1, y; \sigma^*) \, \mathrm{d}y &= \int_0^{1/2} \left(-\chi_0 \phi_{By} + \psi_{0y} \phi_{Byy} \right) \bar{\phi}(1, y; \sigma^*) \, \mathrm{d}y \\ &= -\int_0^{1/2} \left[\chi_0 \phi_{By} + \phi_B \left(\Omega_B \frac{K_0 K_{0y}}{2y^2 \psi_{0y}} + \chi_{0y} \right) \right] \bar{\phi}(1, y; \sigma^*) \, \mathrm{d}y. \end{aligned} \tag{B 23}$$

Combining (B 20)–(B 23), we have

$$E_{ww_{outlet}} = -\frac{1}{2}\epsilon_1^2 \,\mathrm{e}^{2\sigma^* t^*}\left[\frac{1}{2}\int_0^{1/2}\left(\Omega_B \frac{K_0 K_{0y}}{2y^2\psi_{0y}} + \frac{1}{2}\chi_{0y}\right)\phi_B^2 \,\mathrm{d}y A^2(1;\sigma^*)\right.$$
$$+\epsilon\int_0^{1/2}\left(\chi_0\phi_{By} + \chi_{0y}\phi_B + \Omega_B\frac{K_0K_{0y}}{2y^2\psi_{0y}}\phi_B\right)\bar{\phi}(1,y;\sigma^*)\,\mathrm{d}y A(1;\sigma^*)$$
$$\left.+ O(\epsilon^2) + \cdots\right]. \tag{B 24}$$

7. $E_{wp_{outlet}}$: Let $p_1(x,y,t) = \epsilon_1 \bar{p}_1(X,y;\sigma^*)\,\mathrm{e}^{\sigma t}$ be the pressure perturbation. Using this and the axial and radial velocity perturbations $u_1 = \epsilon_1\bar{u}_1\,\mathrm{e}^{\sigma t} + \cdots$ and $w_1 = \epsilon_1\bar{w}_1\,\mathrm{e}^{\sigma t} + \cdots$ in the linearized axial momentum equation $w_{1t} + w_{0r}u_1 + w_0 w_{1x} = -p_{1x}$ gives at order ϵ_1:

$$\sigma\bar{w}_1 + w_{0r}\bar{u}_1 + w_0\bar{w}_{1x} = -\bar{p}_{1x}. \tag{B 25}$$

Substituting (B 1), $X = \sqrt{\epsilon}x$, and $\sigma = \sigma^*\epsilon^{3/2}$ in (B 25) gives

$$\bar{p}_{1X} = -(\phi_B\chi_0 A_X + \psi_{0y}\phi_{By}A_X) - \epsilon\left[\sigma^*\phi_{B_y}A + \bar{\phi}_X\chi_0 + \psi_{0y}\bar{\phi}_{yX}\right] + O(\epsilon^2). \tag{B 26}$$

Integrating (B 26) with respect to X from $X=0$ to $X=1$ gives

$$\bar{p}_1(1,y;\sigma^*) - \bar{p}_1(0,y;\sigma^*) = -(\phi_B\chi_0 + \psi_{0y}\phi_{By})A(1;\sigma^*)$$
$$-\epsilon\left[\sigma^*\phi_{By}\int_0^1 A\,\mathrm{d}X + \bar{\phi}(1,y;\sigma^*)\chi_0 + \psi_{0y}\bar{\phi}_y(1,y;\sigma^*)\right] + O(\epsilon^2). \tag{B 27}$$

Moreover, the linearized radial momentum equation $u_{1t} + w_0u_{1x} - 2\omega v_0 v_1/r = -p_{1r}$ and the inlet conditions $u_{1x}(0,y,t)=0$, $v_1(0,y,t)=0$ show that $p_{1y}(0,y,t) = -u_{1t}(0.y,t)/\sqrt{2y}$. Since $u_1 = \epsilon_1\bar{u}_1\,\mathrm{e}^{\sigma t} + \cdots$ and $\sigma = \sigma^*\epsilon^{3/2}$ we find that $\bar{p}_1(0,y;\sigma^*) = O(\epsilon^2)$. Therefore, it can be neglected in the expression for $\bar{p}_1(1,y;\sigma^*)$ in (B 27).

Inserting $\bar{w}_1$ from (B 1) and $\bar{p}_1$ from (B 27) in (5.8) and retaining the terms up to order $O(\epsilon)$ gives

$$E_{wp_{outlet}} = -\epsilon_1^2\,\mathrm{e}^{2\sigma^* t^*}\left[\int_0^{1/2}\bar{w}_1(1,y;\sigma^*)\bar{p}_1(1,y;\sigma^*)\,\mathrm{d}y\right]$$
$$= \epsilon_1^2\,\mathrm{e}^{2\sigma^* t^*}\left[\int_0^{1/2}(\phi_{By}A(1;\sigma^*) + \epsilon\bar{\phi}_y(1,y;\sigma^*) + O(\epsilon^2))\right.\Big[(\phi_B\chi_0 + \psi_{0y}\phi_{By})A(1;\sigma^*)$$
$$\left.+\epsilon\left(\sigma^*\phi_{By}\int_0^1 A\,\mathrm{d}X + \bar{\phi}(1,y;\sigma^*)\chi_0 + \psi_{0y}\bar{\phi}_y(1,y;\sigma^*)\right)\Big]\mathrm{d}y + O(\epsilon^2)\right] + \cdots. \tag{B 28}$$

Integrating by parts and using the boundary conditions for ϕ_B and the inlet conditions for A results in

$$E_{wp_{outlet}} = \epsilon_1^2 \, \mathrm{e}^{2\sigma^* t^*} \left\{ \Omega_B \left(\int_0^{1/2} \frac{K_0 K_{0y} \phi_B^2}{2y^2 \psi_{0y}} \right) \mathrm{d}y A^2(1;\sigma^*) \right.$$
$$+ \epsilon \left[\sigma^* \left(\int_0^{1/2} \left(\Omega_B \frac{K_0 K_{0y}}{2y^2 \psi_{0y}^2} + \frac{\chi_{0y}}{\psi_{0y}} \right) \phi_B^2 \, \mathrm{d}y \right) \left(A(1;\sigma^*) \int_0^1 A \, \mathrm{d}X \right) \right.$$
$$\left. \left. + \left(\int_0^{1/2} \left(2\chi_0 \phi_{By} + \phi_B \left(\Omega_B \frac{K_0 K_{0y}}{y^2 \psi_{0y}} + \chi_{0y} \right) \right) \bar{\phi}(1, y;\sigma^*) \, \mathrm{d}y \right) A(1;\sigma^*) \right] \right.$$
$$\left. + O(\epsilon^2) \right\} + \cdots . \tag{B 29}$$

REFERENCES

Antkowiak, A. & Brancher, P. 2004 Transient growth for the Lamb–Oseen vortex. *Phys. Fluids* **16**, L1–L4.

Arnold, V. I. 1989 *Mathematical Methods of Classical Mechanics*, 2nd Edn. Graduate Texts in Mathematics, vol. 60. Springer.

Ash, R. L. & Khorrami, M. R. 1995 Vortex stability. In *Fluid Vortices*, chap. 8 (ed. S. I. Green), pp. 317–372. Kluwer.

Benjamin, T. B. 1962 Theory of the vortex breakdown phenomenon. *J. Fluid Mech.* **14**, 593–629.

Drazin, P. G. 2002 *Introduction to Hydrodynamic Stability*. Cambridge Texts in Applied Mathematics. Cambridge University Press.

Fabre, D., Sipp, D. & Jacquin, L. 2006 Kelvin waves and the singular modes of the Lamb–Oseen vortex. *J. Fluid Mech.* **551**, 235–274.

Gallaire F. & Chomaz, J.-M. 2004 The role of boundary conditions in a simple model of incipient vortex breakdown. *Phys. Fluids* **16** (2), 274–286.

Gallaire F., Chomaz J.-M. & Huerre P. 2004 Closed-loop control of vortex breakdown: a model study. *J. Fluid Mech.* **511**, 67–93.

Heaton, C. J. & Peake, N. 2007 Transient growth in vortices with axial flow. *J. Fluid Mech.* **587**, 271–301.

Howard L. N. & Gupta, A. S. 1962 On the hydrodynamics and hydromagnetic stability of swirling flows. *J. Fluid Mech.* **14**, 463–476.

Leclaire, B. & Sipp, D. 2010 A sensitivity study of vortex breakdown onset to upstream boundary conditions. *J. Fluid Mech.* **645**, 81–119.

Leibovich, S. & Stewartson, K. 1983 A sufficient condition for the instability of columnar vortices. *J. Fluid Mech.* **126**, 335–356.

Leibovich, S. 1984 Vortex stability and breakdown: survey and extension. *AIAA J.* **22**, 1192–1206.

Lessen, M., Singh, P. J. & Paillet, F. 1974 The stability of a trailing line vortex. Part 1. Inviscid theory. *J. Fluid Mech.* **63**, 753–763.

Mayer, E. W. & Powell, K. G. 1992 Viscous and inviscid instability of a trailing vortex. *J. Fluid Mech.* **245**, 91–114.

Pradeep, D. S. & Hussain, F. 2006 Transient growth of perturbations in a vortex column. *J. Fluid Mech.* **550**, 251–288.

Rayleigh, Lord 1916 On the dynamics of revolving fluids. *Proc. R. Soc. Lond.* A **93**, 148–154.

Rusak, Z. 1998 The interaction of near-critical swirling flows in a pipe with inlet vorticity perturbations. *Phys. Fluids* **10** (7), 1672–1684.

Rusak, Z., Choi, J. J. & Lee, J. H. 2007 Bifurcation and stability of near-critical compressible swirling flows. *Phys. Fluids* **19**, 114107.

Rusak, Z. & Judd, K. P. 2001 The stability of non-columnar swirling flows in diverging streamtubes. *Phys. Fluids* **13** (10), 2835–2844.

Rusak, Z., Kapila, A. P. & Choi, J. J. 2002 Effect of combustion on near-critical swirling flow. *Combust. Theor. Model.* **6**, 625–645.

Rusak, Z. & Lee, J.-H. 2002 The effect of compressibility on the critical swirl of vortex flows in a pipe. *J. Fluid Mech.* **461**, 301–319.

Rusak, Z. & Lee, J.-H. 2004 On the stability of a compressible axisymmetric rotating flow in a pipe. *J. Fluid Mech.* **501**, 25–42.

Rusak, Z., Wang, S. & Whiting, C. H. 1998 The evolution of a perturbed vortex in a pipe to axisymmetric vortex breakdown. *J. Fluid Mech.* **366**, 211–237.

Schmid, P. & D. Henningson, D. 2001 *Stability and Transition in Shear Flows.* Applied Mathematical Sciences, vol 142. Springer.

Squire, H. B. 1960 Analysis of the vortex breakdown phenomenon. In *Miszallaneen der Angewandten Mechanik*, pp. 306–312. Berlin: Akademie.

Synge, J. L. 1933 The stability of heterogeneous liquids. *Trans. R. Soc. Canada* **27**, 1–18.

Szeri, A. & Holmes, P. 1988 Nonlinear stability of axisymmetric swirling flows. *Phil. Trans. R. Soc. Lond.* A **326**, 327–354.

Wang, S. 2009 On the nonlinear stability of inviscid axisymmetric swirling flows in a pipe of finite length. *Phys. Fluids* **21**, 084104.

Wang, S. & Rusak, Z. 1996 On the stability of an axisymmetric rotating flow in a pipe. *Phys. Fluids* **8** (4), 1007–1016.

Wang, S. & Rusak, Z. 1997*a* The dynamics of a swirling flow in a pipe and transition to axisymmetric vortex breakdown. *J. Fluid Mech.* **340**, 177–223.

Wang, S. & Rusak, Z. 1997*b* The effect of slight viscosity on near-critical swirling flows. *Phys. Fluids* **9** (7), 1914–1927.

Wang, S., Taylor, S. & Ku Akil, K. 2010 The linear stability analysis of Lamb–Oseen vortex in a finite-length pipe. *Trans. ASME: J. Fluids Engng* **132** (3), 1–12.

Wu, J. Z., Ma, H. Y. & Zhou, M. D. 2006 *Vorticity and Vortex Dynamics.* Springer.